metals

MDPI

Review

Hot Ductility, Homogeneity of the Composition, Structure, and Properties of High-Strength Microalloyed Steels: A Critical Review

Alexander Zaitsev [1], Nataliya Arutyunyan [1,2,*] and Anton Koldaev [1]

[1] Bardin Central Research Institute of Ferrous Metallurgy, Moscow 105005, Russia; aizaitsev1@yandex.ru (A.Z.); koldaevanton@gmail.com (A.K.)
[2] Faculty of Chemistry, Lomonosov Moscow State University, Moscow 119991, Russia
* Correspondence: naarutyunyan@gmail.com; Tel.: +7-495-939-1673

Abstract: High-strength microalloyed steels are widely used in various branches of technology and industry due to the simultaneous combination of high indicators of strength, ductility, fatigue, corrosion resistance, and other service properties. This is achieved due to the reasonable choice of the optimal chemical composition and parameters of temperature-deformation treatment of steel that provide a synergistic effect on the dispersed microstructure and characteristics of excess phase precipitates, which control the achievement of these difficult-to-combine properties of rolled products. Additionally, the improvement of the level and stability of these properties, as well as the prevention of the occurrence of defects, is largely determined by the indicators of the homogeneity of the composition, structure by volume and manufacturability of the metal, and primarily hot ductility, which are controlled by the presence of precipitation of excess phases, including microalloying elements. In accordance with the circumstances noted, in the present review, a generalization, systematization, and analysis of the results of the studies are conducted on the effect of phase precipitates on the hot ductility and homogeneity of composition and structure, depending on the chemical composition and parameters of the temperature-deformation treatment of steel.

Keywords: low-carbon microalloyed steels; hot ductility; microstructure homogeneity; composition homogeneity; phase precipitates; carbide; carbonitride

Citation: Zaitsev, A.; Arutyunyan, N.; Koldaev, A. Hot Ductility, Homogeneity of the Composition, Structure, and Properties of High-Strength Microalloyed Steels: A Critical Review. *Metals* **2023**, *13*, 1066. https://doi.org/10.3390/met13061066

Academic Editor: Hardy Mohrbacher

Received: 30 March 2023
Revised: 28 April 2023
Accepted: 30 May 2023
Published: 1 June 2023

1. Introduction

The widespread use of high-strength microalloyed steels is due to a combination of high difficult-to-combine properties: strength, ductility, formability, fatigue, and corrosion resistance, with a relatively simple production technology and low cost. They are used in the manufacture of various vehicles, pipes, building, engineering structures, etc. [1]. The unique set of properties of these steels is ensured by the formation of a finely dispersed homogeneous structure and a system of precipitates of excess phases, including nanosized ones (Figure 1), as a result of a reasonable choice of composition, microalloying system, and parameters of the temperature-deformation treatment of steel. Advances in the development of these steels are based on many studies, summarized in a number of reviews [1–3], including those devoted to a specific microalloying system: Ti [4], Nb [5,6], V [7], and Ti-Mo [8].

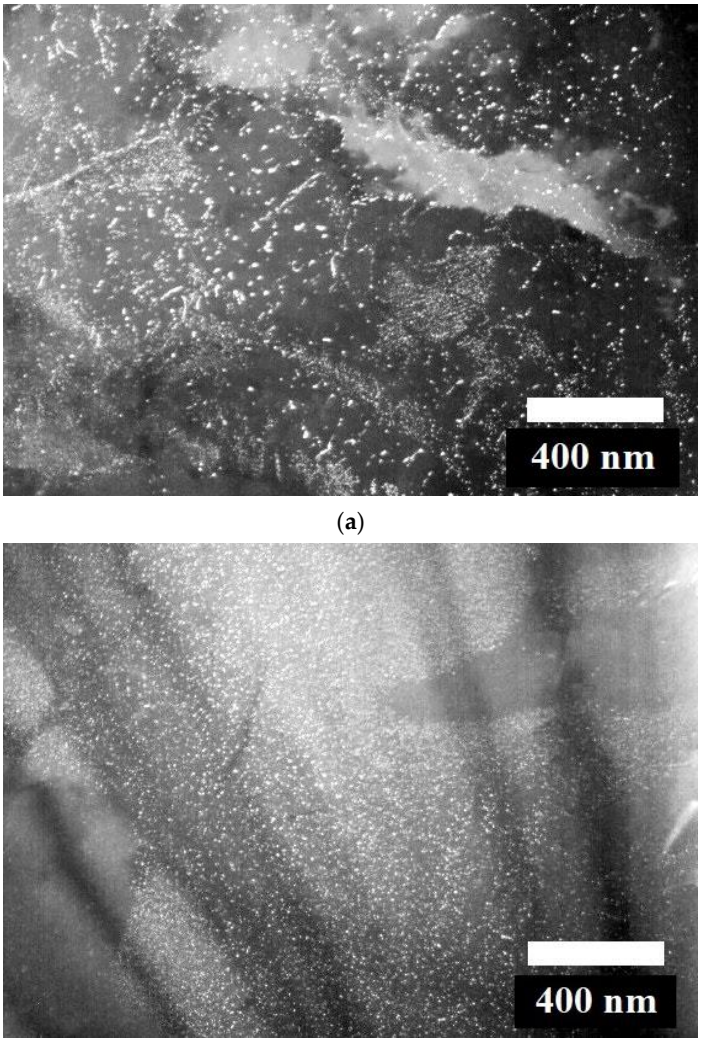

(**a**)

(**b**)

Figure 1. Precipitation of excess phases in high-strength low-carbon microalloyed steels: (**a**) (Ti, Nb)(C, N); (**b**) TiC. Reprinted with permission from ref. [9]. Copyright 2023 Metallurgizdat.

It should be noted that the goal of most studies, and, as a result, reviews, is to achieve maximum strength while maintaining good ductility and a number of other properties [10,11]. However, recently, the attention of researchers has focused on the need to obtain a wider range of properties, including impact toughness [12], fatigue, and corrosion resistance [13], including against hydrogen and hydrogen sulfide cracking [14]. These properties also depend on the presence of precipitates of excess phases, as evidenced by the data in the Table 1. The results of [15] show that NbC nanoscale precipitates act as irreversible hydrogen traps that hinder the accumulation of hydrogen at potential crack nucleation sites. In [12], the deterioration of toughness was established as a result of the formation of a large amount of nanosized, especially interphase, precipitates in Nb, Nb-Mo, and Ti-Mo steels. Fatigue strength at low loads and a low number of cycles is improved due to nanosized precipitates of TiC [16], TiMoC [17], V(C,N) [18], and Fe_3C [19], since cyclic hardening is associated with an increase in density dislocations and the interaction of dislocations with precipitates. At the same time, the level and stability of the obtained properties, including ductility, fatigue strength, and impact strength, directly depend on the homogeneity of the composition and structure over the volume of the metal [20,21]. In addition, in the production of steel products, technological characteristics, such as hot ductility, are of great importance. Hot ductility failure can lead to the premature failure of the metal — the appearance of hot cracks at different stages of the production of metal products.

Table 1. Influence of phase precipitates containing microalloying elements on the properties of high-strength microalloyed steels.

Property	Microalloying System	Effect of Precipitates	Ref.
Strength	Ti	Positive	[4,22]
	Nb		[5,6]
	V		[7]
	Nb-Ti		[9,23–25]
	V-Ti		[26]
	Ti-Mo		[8]
	Ti-Nb-Mo		[9,23,27]
	Ti-Nb-V-Mo		[9]
Impact toughness	Nb, Nb-Mo, Ti-Mo	Negative	[12]
Fatigue strength	Ti	Positive	[16]
	Ti-Mo		[17]
	V		[18]
	Nb-Ti		[19]
Corrosion resistance	Nb	Negative	[28,29]
	V		[28]
Stress corrosion cracking	Nb	Positive	[30]
Hydrogen-induced cracking	Nb	Positive	[15]
Homogeneity	Nb	Negative	[31]
	Nb, Nb-Ti, Nb-V		[32,33]
	Ti-Mo		[33]
Hot ductility	Nb	Depends on size	[34–36]
	Ti, Nb-Ti		[37–40]
	V, Nb-V		[41–44]

This review presents a critical analysis of the data on the effect of precipitates of excess phases on the hot ductility and homogeneity of the chemical composition and microstructure of low-carbon microalloyed steels. In recent decades, considerable experience has been accumulated in ensuring a sufficient level of the hot ductility of steels, which is periodically systematized and summarized in the corresponding reviews [34,35,45,46]. Nevertheless, the technologies of metallurgical production are developing, the requirements for the properties of metallurgical products are increasing, and, therefore, studies of the factors affecting hot ductility are continuing and focusing on specific classes of steels. Reviews have recently been published on studies on the hot ductility of twinning-induced plasticity (TWIP) and transformation-induced plasticity (TRIP) steels [35,47]. However, high-strength microalloyed steels continue to occupy a leading position in terms of production and consumption. Therefore, it is relevant to generalize and analyze the available results of studying the hot ductility of precisely high-strength microalloyed steels, the structural state and properties of which are largely controlled by microalloying elements. Microalloying elements differ from alloying elements, not only in concentration (usually not more than 0.1 wt.%), but also in the physical mechanism of their influence: alloying elements mainly affect the steel matrix, while the influence of microalloying elements is largely associated with the formation of excess phases.

Therefore, when analyzing the influence of microalloying elements, we use the results of a thermodynamic calculation of the regions of existence of the corresponding excess phases conducted in this work and earlier studies. This was performed using a thermodynamic computer model [48], implemented on the basis of proprietary software, by finding the conditions of thermodynamic equilibrium in multicomponent multiphase systems with specified external and internal parameters (temperature, pressure, and composition). The basis of resolving this problem is a search for the nonlinear Gibbs energy functional for a multicomponent multiphase system with linear balanced limitations, i.e., the sum of fractions of the coexisting phases equals one, the sum of molar components in each of these phases also equals one, and, finally, each sum of the products of phase fractions in a molar fraction within the composition of the ith component equals the total molar

fraction of this component within a system. For the approximation of the thermodynamic properties of phases of variable composition, a generalized sublattice model is used [49,50], taking account of the magnetic component of Gibbs energy [51]. The main parameters are borrowed from [52,53].

2. Effect of Precipitates of Excess Phases on Hot Ductility

To consider the features of the effect of excess phase precipitates on the hot ductility of high-strength low-carbon microalloyed steels, it was necessary to first briefly describe the main mechanisms that controlled the change in ductility at high temperatures.

2.1. Main Mechanisms of Ductility Decrease at a High Temperature

One of the most common methods for studying the ductility of steels at high temperatures is the measurement of the reduction in area (RA, %) of samples by tensile tests in the required temperature range, followed by the performance of the so-called hot ductility curves. The typical temperature dependence of ductility (RA) has a trough that starts at about 700 °C and can increase to the solidus temperature. Figure 2 shows the temperature dependences of RA with a plasticity trough and the corresponding microphotography of fractures.

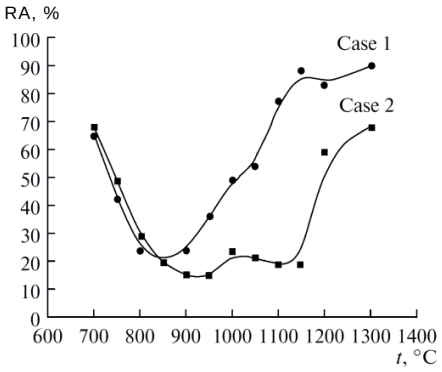

(**a**)

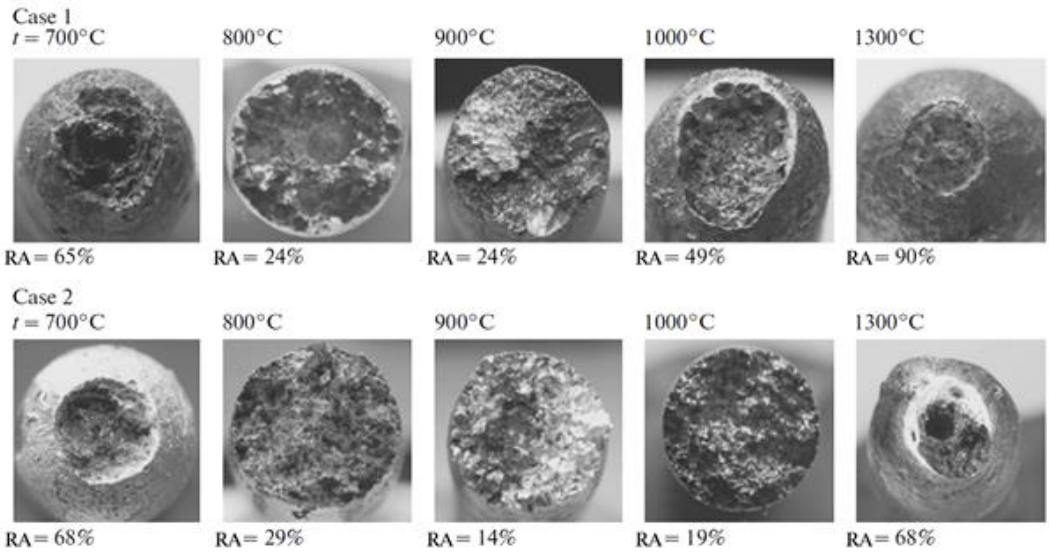

(**b**)

Figure 2. (**a**) Temperature dependences of reduction in area; (**b**) corresponding microphotography of fractures for steel containing wt.%: 0.1 C, <1.2 (Mn + Si), 0.06 Cu, 0.04 Al, <0.03 (Nb + V + Ti), 0.005 S, 0.006 N. Reprinted with permission from ref. [54]. Copyright 2023 Stal'.

The reasons for this phenomenon are due to a number of mechanisms, the implementation of which depends on the temperature interval. The authors of [55–57] distinguished three regions of ductility troughs in steels. Region 1 is at high temperatures, typically 20–50 °C below the mean solidus temperature [56]. Fracture surfaces are characterized by interdendritic fractures and the presence of precipitates, such as MnS. The low ductility in this region is associated with the formation of a liquid layer at the interdendritic boundaries and along the boundaries of austenite grains. In region 1, ductility does not depend on the intensity of deformation, but mainly depends on the chemical composition, in particular, on microsegregations of sulfur, manganese, and phosphorus [56].

Region 2 is between 900 and 1200 °C, depending on the composition and test conditions. This region is associated with intergranular fractures. The fracture edges are either covered with small dimples or microvoids, or they are smooth. This suggests two different mechanisms. In the first case, in areas close to the grain boundary, the deformation initiates the formation of voids at the grain boundaries, inclusions, or precipitates, which leads to intergranular fractures due to the merging of microvoids. In the second case, slip occurs along the grain boundaries in a single-phase austenite region, followed by wedge-shaped cracking.

Most often, region 2 is characterized by the formation of small intergranular precipitates of sulfides, oxides, and carbonitrides along the boundaries of austenite grains. This leads to the appearance of so-called "soft zones" — precipitate-free zones (PFZs) along the boundaries of austenite grains on both sides of the boundaries (width 500 nm), or to the formation of microcavities around precipitates and their subsequent coalescence [45,56]. Precipitate-free zones are places of strain concentration, which leads to failure, even for small strains in the continuous casting of steel [55].

In [56], this region was subdivided into two, depending on the stability of various types of precipitates and, accordingly, the mechanisms of ductility reduction. In region IIa, (Mn, Fe)S and MnS precipitates play the main role; in region IIb — Nb(CN), V(CN), Ti(CN), and AlN.

Such a division can be clearly explained from a thermodynamic analysis of the regions of existence of phases in the steels under consideration [48]. Figure 3 shows the results of the thermodynamic calculation for the steel of a model composition microalloyed with niobium. It can be seen that the precipitation of MnS begins at higher temperatures than Nb(CN).

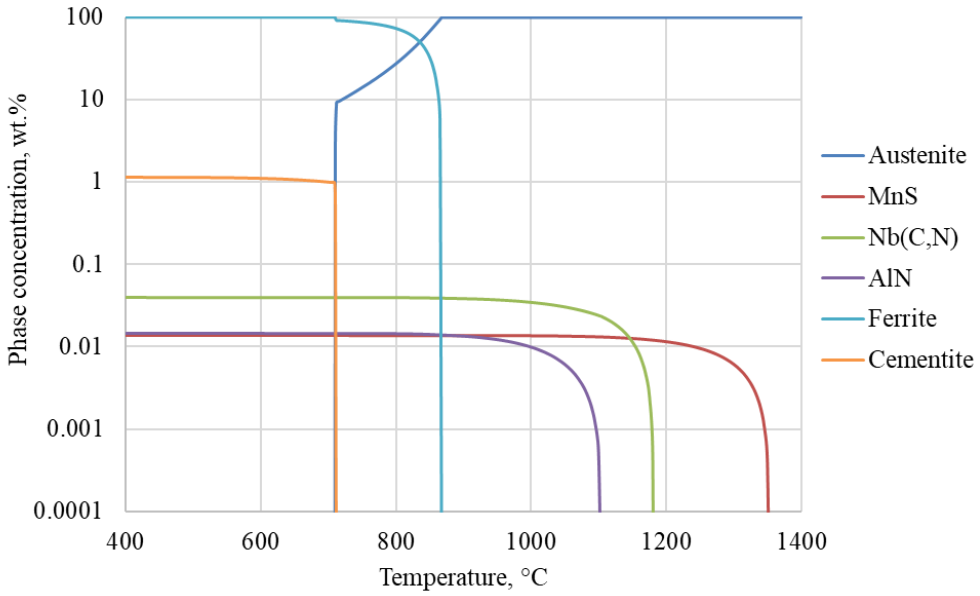

Figure 3. Temperature dependence of the phase composition of steel containing wt.%: 0.08 C, 0.60 Mn, 0.10 Si, 0.045 Al, 0.005 S, 0.005 P, 0.005 N, 0.035 Nb.

Low ductility in region IIa is detected only at sufficiently high strain rates, while in region IIb, ductility worsens with a decreasing strain rate. In region IIa, at lower strain rates or at long holding times before testing, the ductility is quite good [56,58].

Ductility decreasing in region IIa is highly dependent on the composition, in particular, on the Mn/S ratio. In [59], it was suggested that the ductility loss in this case is due to the segregation of S at the boundaries of austenite grains.

Ductility loss in region IIb is initiated by slip along austenite grain boundaries [45,60] and the presence of precipitates of excess phases, such as Nb(CN), V(CN), or AlN. These precipitates play two main roles: they can delay the onset of recrystallization and reduce the stress required for failure.

The authors of reviews [45,56,57] noted that ductility failure in the temperature range of 1000–1150 °C may be associated with a delay in dynamic recrystallization, especially in microalloyed steels. It is well known that microalloying elements, especially niobium, can delay recrystallization [5,61]. If recrystallization can occur before fracture, any developing cracks along the grain boundaries become isolated and no further propagation is possible. Due to the absence of dynamic recrystallization, the austenite grain size increases, thereby reducing the total length of the boundaries, increasing the concentration of inclusions and precipitates along the boundaries of austenite grains. In turn, this leads to intergranular fracture.

The decrease in the fracture stress in the presence of precipitates of microalloying elements can occur through a number of possible mechanisms. First, precipitate-free zones are often observed near austenite grain boundaries, which can lead to strain concentration at the grain boundary. Second, particles (or groups of particles) at grain boundaries can act as crack initiation sites. In addition, the formation of inclusions and precipitates throughout the matrix can lead to an increase in strength and a general decrease in ductility [45,46].

As mentioned above, intergranular fracture can occur not only due to the merging of microvoids, but also through sliding along grain boundaries, which is due to plastic deformation of austenite grain boundaries [45]. The destruction of the grain boundary occurs when the stresses in the triple junctions of the grains exceed the maximum allowable stress. This failure mechanism is usually associated with creep. As a rule, this takes place at strain rates below 10^{-4} s^{-1}. However, cracks characteristic of grain boundary slip failure are often found at the strain rate commonly used in hot tensile testing (10^{-3} s^{-1}).

Grain boundary slip is enhanced by the presence of various precipitates at the austenite grain boundaries [45]: sulfides, oxides, nitrides and/or carbides act as stress concentrators and promote crack formation. If the stress concentration at such grain boundary particles is produced by grain boundary sliding alone, the dislocation pile-up distance corresponds to the interparticle spacing, so that large applied stresses are required for particle fracture or particle–matrix decohesion. However, for the case of intergranular slip band impingement against a grain boundary particle, much smaller applied stresses are required for particle fracture, since the slip distances are much greater [45].

Region 3 is in the low temperature range of austenite existence, including the austenite to ferrite transformation, and occurs over the approximate temperature range 600–900 °C, depending on the chemical composition of the steel. It is believed that this region of low ductility is associated with the austenite to ferrite transformation. On cooling below the transformation temperature, the formation of ferrite begins at the boundaries of the austenite grains, leading to the formation of ferrite films around the austenite grains with a thickness of 5–20 μm [45]. At temperatures within the transformation range, ferrite is softer than austenite; therefore, there is a concentration of strain within the ferrite along the grain boundaries. The nucleation of voids on phase precipitates (often MnS) are located at the boundaries of austenite grains, and the growth of these voids continues inside the ferrite film.

Strain-induced ferrite can form at temperatures above the undeformed A_{r3} temperature (the transformation start temperature at a constant cooling rate) and often reaches A_{e3}, since the deformation process accelerates the transformation kinetics [62]. Below the A_{e3}

temperature, the ferrite thickness does not change significantly with temperature [62] until the A_{r3} value is reached. At temperatures just below A_{r3}, there is a thickening of the ferritic films and/or a decrease in the relative differences in strength between the austenite and ferrite phases. Further lowering the test temperature rapidly thickens the ferrite film and the ductility recovers completely when ~50% ferrite is present prior to testing.

Review [45] summarized the following explanations for the accelerating effect of deformation on the nucleation rate of ferrite:

(a) Deformation causes local grain boundary migration leading to bulges at the austenite boundaries, which act as nuclei;
(b) Subgrains are formed near the boundaries, which locally increase the stored energy;
(c) Increased dislocation density in the deformed austenite increases the strain energy, promoting ferrite nucleation.

Thus, the failure of hot plasticity can be caused by various mechanisms depending on the temperature range. As the temperature decreases, these mechanisms can be arranged in the following order:

- Formation of a liquid layer at the interdendritic boundaries and along the boundaries of austenite grains;
- Formation of (Mn,Fe)S along the boundaries of austenite grains;
- Formation of precipitates of excess phases (Nb(CN), AlN, V(CN), etc.) along the boundaries of austenite grains;
- Inhibition of dynamic recrystallization of austenite;
- Sliding along the grain boundaries;
- Formation of zones free from precipitation of dispersed particles adjacent to the boundaries of austenite grains;
- Formation of the ferrite film along the boundaries of austenite grains.

The implementation of all these mechanisms depends both on the chemical composition of the steel and on the deformation conditions, parameters that also control the formation and growth of phase precipitates.

2.2. Effect of Sulfides

A detailed review of the effect of sulfur on hot ductility is given in [45]. According to the general opinion of researchers, sulfur worsens the hot ductility of steels. In this case, the degree of effect depends both on the form and on the place where sulfur is present: grain boundaries or matrix. This causes the implementation of various embrittlement mechanisms, which are summarized in Table 2. First of all, the weakening of the strength of the austenite grain boundaries can be caused by the segregation of sulfur at the grain boundaries [59,63]. For high-strength microalloyed steels, the hot ductility is dominated by sulfides precipitated along the austenite grain boundaries. Any sulfides present in the matrix have little effect on hot ductility. In this case, the Mn/S ratio plays an important role [63–67].

At a low manganese content, a FeS phase with a low melting temperature forms as a liquid interlayer along the grain boundaries, causing intergranular fracture [66]. The implementation of this embrittlement mechanism is determined by several factors. The mobility of sulfur is about 1000 times greater than the mobility of manganese at 1090 °C. Therefore, upon rapid cooling to a temperature below the solubility limit of sulfur in pure iron, metastable FeS will form at the grain boundaries. At lower cooling rates, manganese has time to diffuse to the grain boundaries and the FeS precipitates will be enriched in Mn. At a sufficiently slow cooling rate, stable MnS will be nucleated. A continuous flat array of small solid particles or small liquid droplets along the grain boundary can result in low ductility and serve as an easy path for crack propagation.

Table 2. Influence of the form of presence of sulfur on the hot ductility failure.

Form of Presence	Mechanism	Features of the Conditions	Ref.
S	Segregation along grain boundaries	High temperatures, 20–50 °C below solidus	[59,63]
FeS	Liquid layer along the grain boundaries	Low Mn/S ratio, high cooling rate	[66]
(Fe,Mn)S	Finely dispersed precipitates along the grain boundaries. Formation of PFZs	Low Mn/S ratio, medium cooling rate	[58,66,68]
MnS	Finely dispersed precipitates along the grain boundaries. Formation of PFZs	Low Mn/S ratio, low cooling rate	[59,66,69]

As the Mn/S ratio increases, the hot ductility improves, but the ductility trough remains and the embrittlement mechanism changes. Very small (Fe,Mn)S and MnS precipitates are formed at the boundaries of austenite grains, which leads to the appearance of microcavities around the precipitates (PFZs) and their subsequent coalescence [45,58,68]. Finely dispersed segregations of sulfides inside the grains and the presence of PFZs along the grain boundaries enhance the localization of deformation near the boundaries during deformation. According to [45], the favorable effect of increasing the Mn/S ratio above 2 or 3 by lowering the sulfur level is attributed to a decrease in the volume fraction of MnS inclusions. In [69], to reduce precipitation at grain boundaries, it is recommended to use Ca and/or Ce additives, which cause precipitation of sulfides in the melt.

As the Mn/S ratio is further increased up to 60, the hot ductility continues to improve [66,70]. According to [66], there is an additional positive factor. With an increase in manganese content, the driving force of MnS precipitation increases, contributing to its precipitation in the matrix, and not at a more harmful place—austenite boundaries.

2.3. Effect of Niobium Carbonitride

According to many studies, steels containing niobium are highly susceptible to transverse cracking during continuous casting [34,36,40,55,56,68,71–73]. The works [34,36] indicate three main reasons:

1. Niobium has a strong effect on reducing the A_{r3} temperature that expands the trough in the low temperature interval.
2. The precipitation of Nb(CN) in a finely dispersed form during the deformation of austenite in the temperature range of the straightening operation facilitates the connection of cracks, which leads to intergranular fracture. Precipitation also widens the trough in the higher temperature interval.
3. Larger NbCN precipitates at the austenite grain boundaries cause the formation of precipitate free zones. As a result, poor ductility persists at temperatures above A_{e3}; therefore, the trough expands in the high temperature interval.

Reducing the carbon content in Nb-containing steels leads to a decrease in the amount of harmful precipitates and, thereby, improves hot ductility. However, above 0.1% C, niobium has only a negligible detrimental effect on hot ductility [72]. Not only the amount of precipitates, but also their composition depends on the nitrogen content. The greater the N/C ratio in the steel, the more nitrogen there is in the carbonitride [5]. In [72], it was shown that, at a low nitrogen level (0.002% N), niobium carbide was formed, resulting in good ductility; at higher levels (0.006% N), niobium carbonitride was formed and the ductility deteriorated markedly. It has been suggested that this was due to the easier precipitation of Nb(CN) compared to NbC in the higher temperature region where the straightening operation occurs.

Indeed, as studies show, at higher temperatures, a more nitrogen-saturated carbonitride is formed [5]. Figure 4 shows the results of the thermodynamic calculation of the temperature of formation of niobium carbonitride precipitates at various Nb and N contents conducted using a computer program [48] for steel of basic composition, wt.%: 0.08 C–0.60 Mn–0.10 Si–0.045 Al–0.005 S–0.005 P. It can be seen that, with an in-

crease in the nitrogen content at each given concentration of niobium, the temperature of the beginning of Nb(CN) precipitation increases.

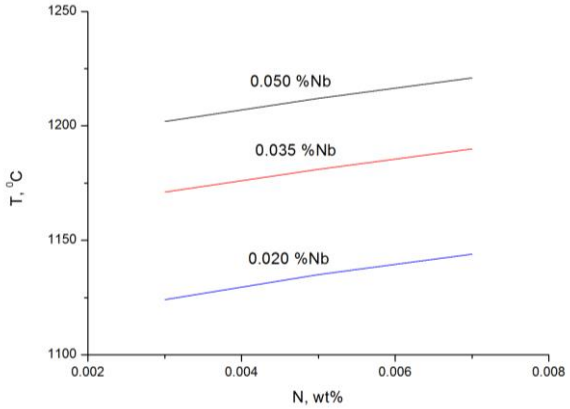

Figure 4. Temperature of the beginning of Nb(CN) precipitation depending on the concentration of nitrogen and niobium during cooling. The base composition of steel, wt.%: 0.08 C–0.60 Mn–0.10 Si–0.045 Al–0.005 S–0.005 P.

The presence of strong nitride-forming elements, such as titanium and aluminum, in the composition of steel affects both the composition of niobium carbonitride and the temperature of its formation. In addition, it was found in [74] that the hot ductility of Nb-microalloyed steel is improved by adding 0.12 wt.% Cr. Chromium atoms prevent the diffusion of carbon atoms, which reduces the thickness of the grain boundary ferrite. The number of fractions of high-angle grain boundaries increases with increasing chromium content, which prevents the propagation of cracks and improves the ductility of the steel.

2.4. Effect of Titanium Nitride and Carbonitride

Studies of the titanium effect on the hot ductility of steels were conducted in many works, including [37–39,56,75,76]. It was found that this influence can be both positive and negative. Table 3 summarizes the results of the works [37–39,75,76].

The main factor that improves hot ductility is the precipitation of titanium nitride at a high temperature. These particles, on the one hand, are larger; on the other hand, they serve as a substrate for the subsequent precipitation of niobium carbonitride. As a result, the size of the precipitates present in the microstructure is larger and their quantity is reduced. This can be clearly explained from a thermodynamic analysis of the regions of phase existence in the steels under consideration. Figure 5 shows the results of a thermodynamic calculation of the equilibrium phase composition of steels containing, wt.%: 0.8 Mn, 0.3 Si, 0.045 Al, and 0.007 N with varying concentrations of C (0.08 and 0.11), Nb (0.02, 0.04, and 0.07), Ti (0.010 and 0.025), and V (0.05 and 0.07). It can be seen that Nb(C,N) precipitation during cooling begins much later than TiN. In addition, according to the results of [77], the formation of carbide, carbonitride precipitates of niobium, even during deformation, is kinetically inhibited. Therefore, in the absence of titanium, the formation of more dispersed niobium precipitates occur.

An Investigation of two Nb-microalloyed steels showed that the addition of 0.015 wt.% Ti significantly improves hot ductility from a minimum RA value of 19.4% at 750 °C to 41.4% at 800 °C [39]. The failure of hot plasticity is mainly associated with the formation of a ferrite films at the boundaries of austenite grains. In steel without titanium, Nb(C,N) precipitates form at the grain boundaries, which greatly increase the sensitivity to cracking and leads to a failure of hot ductility. When titanium is added, only (Ti, Nb)(C, N) particles are observed inside the grain. In this case, (Ti, Nb)(C, N) nucleation occurs on the surface of the existing TiN precipitates.

Table 3. Effect of titanium on the hot ductility of low-carbon steels.

Chemical Composition, wt.%										Effect	Cooling	Ref.
C	**Si**	**Mn**	**Al**	**S**	**P**	**Nb**	**N**	**Ti**	**Fe**			
0.06	-	1.6	0.021	-	-	0.035	0.006	0.006	Bal.	Positive	900 K/min	[76]
0.03–0.04	-	1.6	-	-	-	0.03	0.0042–0.0077	0.012–0.013	Bal.	Negative	300 K/min	[37]
0.04–0.05	-	1.6	-	-	-	0.013–0.016	0.0044–0.0081	0.01	Bal.	Negative		[37]
0.04–0.05	-	1.6–1.72	-	-	-	0.044–0.055	0.0048–0.0072	0.013–0.036	Bal.	Negative		[37]
0.04–0.05	-	1.6	-	-	-	0.013–0.016	0.0044–0.0081	0.01	Bal.	Weakly positive	Cooling—heating—cooling	[37]
0.04–0.05	-	1.6–1.72	-	-	-	0.044–0.055	0.0048–0.0072	0.013–0.036	Bal.	Positive		[37]
≤0.15	0.14–0.15	<2	0.039–0.054	-	-	0.041–0.042	Not specified	0.015	Bal.	Positive	300 K/min	[39]
0.11	0.32–0.38	1.48–1.54	0.023–0.035	0.004	0.015–0.019	0.023–0.029	0.008–0.009	0.02	Bal.	Positive	25 K/min	[75]
0.051–0.052	0.37–0.38	1.51	0.030	0.009–0.010	0.014–0.015	-	0.0094	0.02	Bal.	Weakly positive	60 K/min	[75]
0.086–0.098	0.31–0.35	1.41–1.44	0.008–0.036	0.002–0.019	0.009–0.019	0.032–0.042	0.0040–0.0110	0.014–0.045	Bal.	Negative	25, 100, 200 K/min	[38]

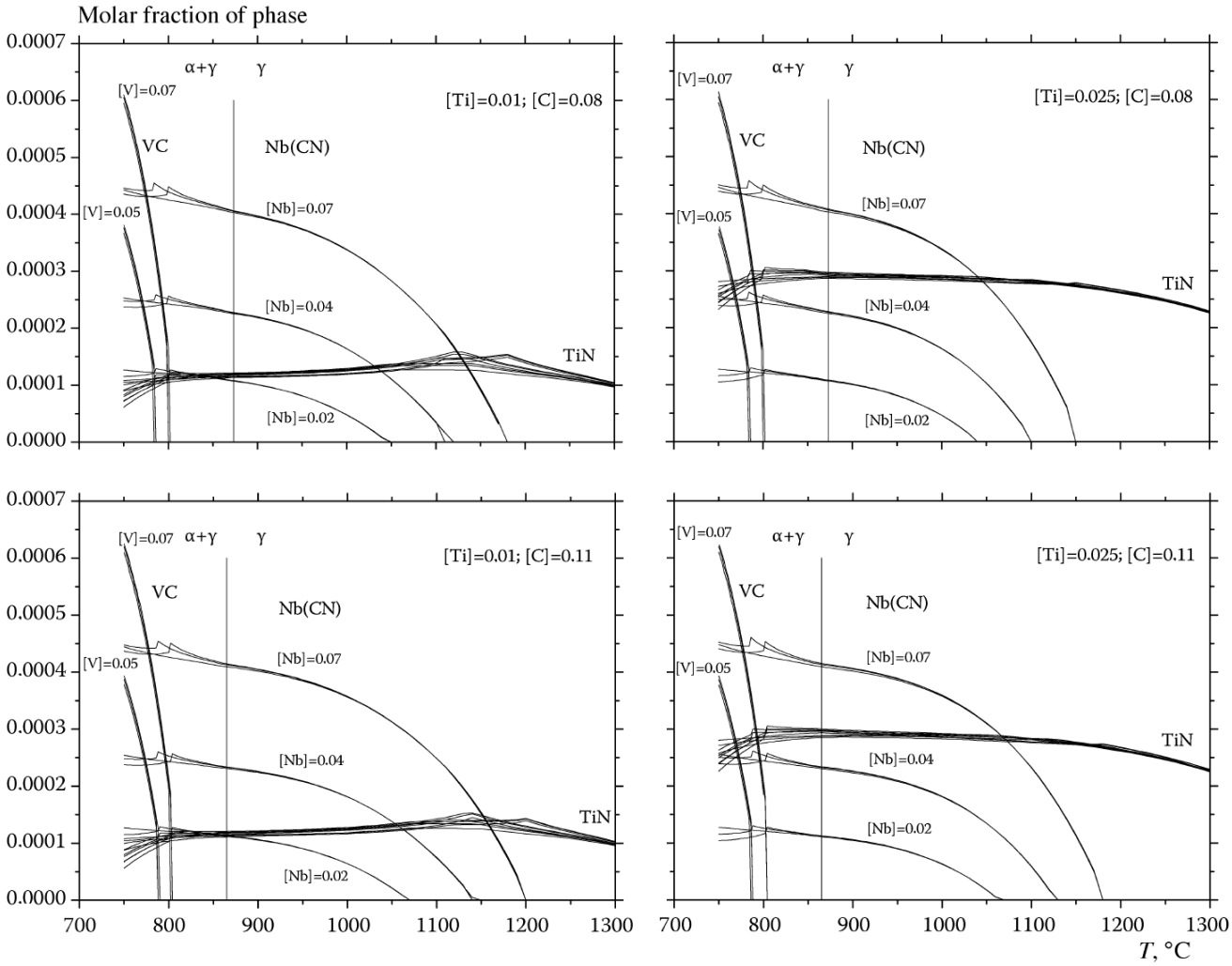

Figure 5. Equilibrium phase composition of steels containing, wt.%: 0.8 Mn, 0.3 Si, 0.045 Al, and 0.007 N. Reprinted with permission from ref. [78]. Copyright 2023 Metallurgizdat.

Similar results were obtained in [75] when studying the distribution of precipitates at a cooling rate of 25 K/min: large TiN particles serve as a substrate for the precipitation of niobium at high temperatures. As a result, there remains a smaller amount of niobium available for precipitation during deformation in the temperature range of 800–1000 °C. In addition, in steels containing aluminum, the formation of TiN prevents the precipitation of more harmful AIN and contributes to the improvement of ductility, which was observed in [75] at a cooling rate of 60 K/min.

In contrast to the results [39,75] in [38], even at a cooling rate of 25 K/min, titanium had a negative effect on the hot ductility of Nb-microalloyed steels. The levels of titanium and nitrogen varied within 0.014–0.045 and 0.004–0.011 wt.%, respectively, which made it possible to study a wide range of Ti/N ratios. An improvement in hot ductility was observed with coarsening precipitates due to a decrease in the cooling rate and an increase in the Ti/N ratio above the stoichiometric one, which increases the amount of Ti in solution and promotes particle growth.

Thus, when large TiN precipitates may form, such as in the case of low cooling rates or high Ti/N values, hot ductility can be slightly improved by titanium addition. However, under conditions where a high volume fraction of TiN fine particles is formed, such as the stoichiometric Ti/N ratio in low-nitrogen steels, hot ductility may deteriorate when titanium is added [56]. In addition, as noted in [56], when studying the effect of titanium

on hot ductility, it is important to take into account the size of the austenite grain, since, when adding titanium, an increase in hot ductility can occur due to a decrease in grain size.

In addition to the previous studies, in [37,79], it was shown that the effect of titanium on Nb-microalloyed steels depends on the cooling conditions. The ductility of Ti-containing steels, upon melting and cooling, to the test temperature at a constant cooling rate, as a rule, decreased due to the appearance of smaller and more numerous Ti-containing precipitates. At the same time, under production conditions, a positive effect of titanium is observed. The difference between the cooling mode under production conditions is as follows. In the commercial casting operation, the primary cooling underneath the mold is very rapid. The temperature at the foot rolls reaches a minimum, rises again, and then falls gradually during secondary cooling until the unbending temperature is reached. Additional temperature losses are also incurred when the strand passes over the guide rolls. A cooling mode similar to that of industrial continuous casting was used in [37]. In this case, cooling from the melt stability temperature starts rapidly, reaches a minimum, and then reheating occurs, after which the temperature drops more slowly to the test temperature. The use of such a mode led to an improvement in the hot ductility of steels below 900 °C. At the same time, the Ti/N ratio was of great importance. With the addition of 0.01 wt.% Ti, this improvement, although noticeable, resulted in only a slight improvement in ductility compared to steel without Ti, and then only in the temperature range of 800–900 °C. In steel with a high niobium content (>0.03 wt.% Nb), increasing the Ti content to 0.036 wt.% so that the Ti/N ratio is high (7.5/1) resulted in much better ductility in the temperature range of 800–900 °C, while the RA value was 60%. The ductility was now significantly better than the ductility of steel with the same composition, but without titanium.

2.5. Effect of Aluminum Nitride

According to [34], for C-Mn-Al steels with a low N content, by having a C content in the peritectic range (0.10–0.17 wt.% C) with an Al content <0.04 wt.% (solubility product of [Al][N] < 20×10^{-5}) as a rule, there is no significant problem with transverse cracking. An increase in the solubility product of [Al][N] leads to both the deepening and widening of the through. A significant negative effect of aluminum is observed when [Al][N] exceeds 30×10^{-5}.

The hot ductility of Al-containing steels in the as-cast state can often be worse than when examining samples after solution treatment (1350 °C). This appears to be because casting results in the segregation of Al towards the boundaries, and high supersaturation promotes AlN precipitation there, a situation that is not present when samples' tensile specimens are only solution-treated. In [80], AlN precipitation was observed in a slab made of steel with composition, wt.%: 0.1–0.2 C, 0.3–0.4 Si, 1.0–2.0 Mn, <0.02 P, <0.015 S, <0.04 Al. AlN particles precipitate at the grain boundary and inside the grains when the steel is cooled. As the temperature increased, the AlN precipitates' size increased and the number of AlN precipitates decreased. The most intense formation of AlN precipitates with a size of about 20 nm occurred at 850 °C. At the same time, hot plasticity was the lowest: RA was 15%.

The work [45] considered the implementation of two embrittlement mechanisms in the case of the influence of aluminum. At the high-temperature end of the through, the samples with cracks showed intergranular fractures with flat faces and no signs of coalescence of microvoids or ferrite formation. Therefore, it was assumed that embrittlement occurred due to the slip of grain boundaries in austenite, which was accompanied by the initiation of cracks at triple points. In the case of steels with high [Al][N] product, it was likely that AIN precipitates formed at the austenite grain boundaries, pinning them and allowing grain boundary slip cracks to join. Lowering the temperature below A_{e3} leads to strain-induced ferrite, resulting in embrittlement due to the coalescence of microvoids. Thus, in these steels, the ductility trough is the result of both slip along the grain boundaries and the coalescence of microvoids in the ferrite. It is interesting to note that the transition from one type of fracture mechanism to another, as a rule, Is not accompanied by any discontinuity

in the hot plasticity curve, which indicates that both mechanisms involve the same stress intensification at the boundaries.

In Nb-microalloyed steels, the addition of aluminum leads to a marked deterioration in hot ductility [46,73]. It was suggested that the lower ductility obtained with the aluminum addition is not only due to AlN precipitation [46]. The presence of aluminum slows down the precipitation of Nb(CN), which leads to finer Nb(CN) precipitates. Possibly, this is due to the fact that the precipitation of niobium carbonitride is kinetically difficult [77], and the difference in the start temperatures of AlN and Nb(CN) precipitation is small. Figure 6 shows the results of a thermodynamic calculation of the phase composition of two low-carbon steels microalloyed with niobium [81]. It can be seen that the difference in the start temperatures of AlN and Nb(CN) precipitation is only a few tens of degrees. Therefore, it can be assumed that the precipitation of these two phases occurs in competition; therefore, the particles of niobium carbonitride do not have time to grow.

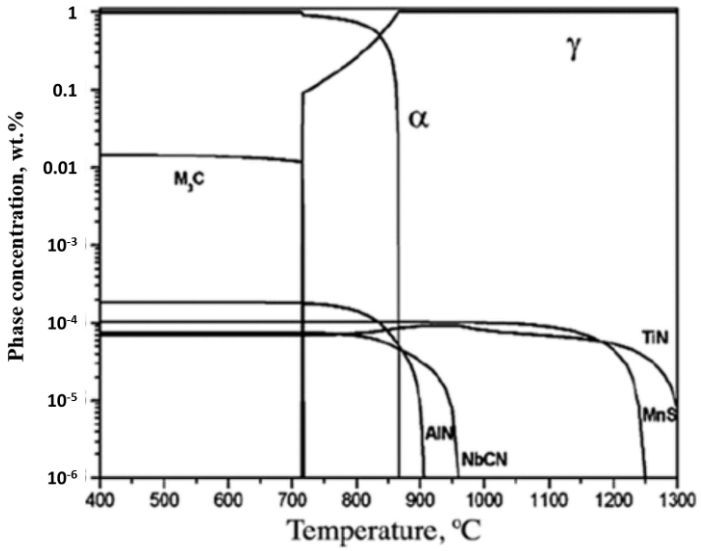

(**a**)

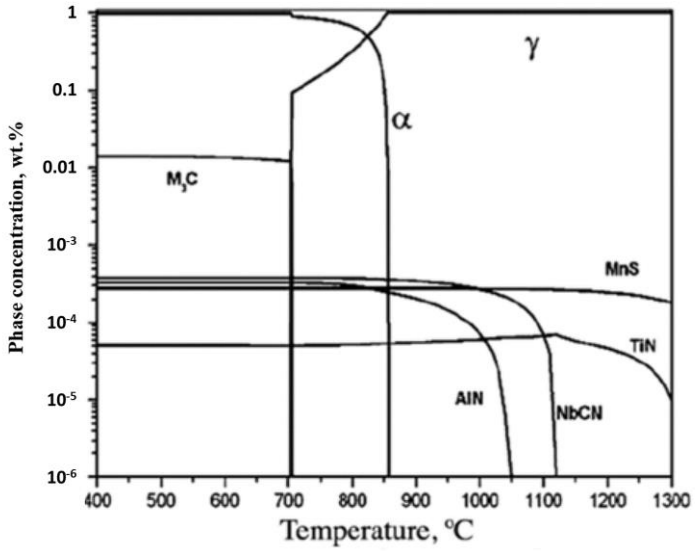

(**b**)

Figure 6. Equilibrium phase composition of steels, wt.%: (**a**) 0.08 C–0.027 Si–0.34 Mn–0.022 Al–0.011 Nb–0.0032 N; (**b**) 0.08 C–0.024 Si–0.71 Mn–0.032 Al–0.032 Nb–0.0048 N. Reprinted with permission from ref. [81]. Copyright 2023 Metallurgizdat.

The study [82] described the symbiotic character of MnS and AlN co-precipitation in the austenitic region of low-carbon steel with composition, wt.%: 0.104 C–0.044 Si–0.43 Mn–0.009 S–0.046 Al–0.025 Cu–0.0009 Ti–0.004 N. The effect of two different heat treatments was investigated: "mild cooling", which simulates the usual cooling conditions for the concast strand and "rapid cooling with reheating". It was shown that almost no MnS/AlN co-precipitation was observed during mild cooling. Instead, only pure MnS precipitates were found, which were predominantly nucleated at dislocations. After rapid cooling with reheating, most precipitates were MnS/AlN co-precipitations on dislocations. In this case, there was a significant widening of the ductility trough compared to the mild-cooling heat treatment.

2.6. Effect of Vanadium Carbonitride

The peculiarity of the influence of vanadium is due to the higher solubility in austenite and the lower temperature of the precipitation of its carbonitride compared to titanium and niobium. Figure 7 shows the calculated phase composition of low-carbon steels for 0.05 wt.% Nb and 0.05 wt.% V. It can be seen that the difference in the temperature of the onset of carbonitride precipitation is about 400 degrees. Due to low temperatures and competition with the simultaneous reaction of cementite formation, V(C,N) precipitation is kinetically inhibited. At the same time, the temperature of the beginning of its precipitation falls within the temperature range of straightening in the industrial production process; therefore, the presence of these particles affects the hot ductility.

With an increase in the vanadium and nitrogen concentration, the temperature of the beginning of the vanadium carbonitride precipitation increases. At the same time, the fraction of nitrogen in its composition increases, approaching VN. As a result, its effect on hot ductility is stronger, approaching that of niobium carbonitride. However, under the same test conditions, the hot ductility of V-containing steels is superior to that of steels with Nb [56]. For example, steel containing 0.16 wt.% V and 0.011 wt.% N had better hot ductility than steel with 0.039 wt.% Nb. This is explained by the fact that vanadium forms a smaller amount of precipitates with nitrogen than niobium. Moreover, the VN particles are larger than the NbCN particles, which is less harmful to the hot ductility of the steel [83]. At the same time, when comparing V-Ti and Nb-Ti microalloyed steels, it was found that both types of steel had the same hot ductility.

The results of [56] show that additions of vanadium up to 0.1 wt.% with a low-nitrogen content (<0.005 wt.%) had only very little detrimental effect on hot ductility by widening the ductility trough. At higher nitrogen levels, the effect of vanadium additions becomes more pronounced and the ductility trough becomes deeper and wider. In [47], it was also noted that the effect of vanadium on the hot ductility of steel was detected only with an increased vanadium content (0.095 wt.%) in a complex with a high nitrogen content (0.014 wt.%).

The authors of [34,46,83,84] attributed the influence of vanadium to the presence of nitrogen in steel. Steels with a carbon content in the peritectic range in the case of V-microalloying had better ductility than 0.03% Nb-containing steels with 0.005 wt.% N, provided that the [V][N] product did not exceed 1.2×10^{-3} (corresponds to 0.1 wt.% V and 0.012 wt.% N). However, an increase in the concentration of vanadium or nitrogen led to a deeper and wider trough with low plasticity, which was due to a large amount of precipitates.

In [85], for steel with 0.07 wt.% V, as the nitrogen concentration increased from 0.0053 to 0.016 wt.%, the ductility trough became wider and deeper. The low ductility intervals were 780–860 °C and 770–920 °C, and the minimum RA value was 47% and 35% at 800 °C, respectively. A similar situation occurred with an increasing vanadium concentration.

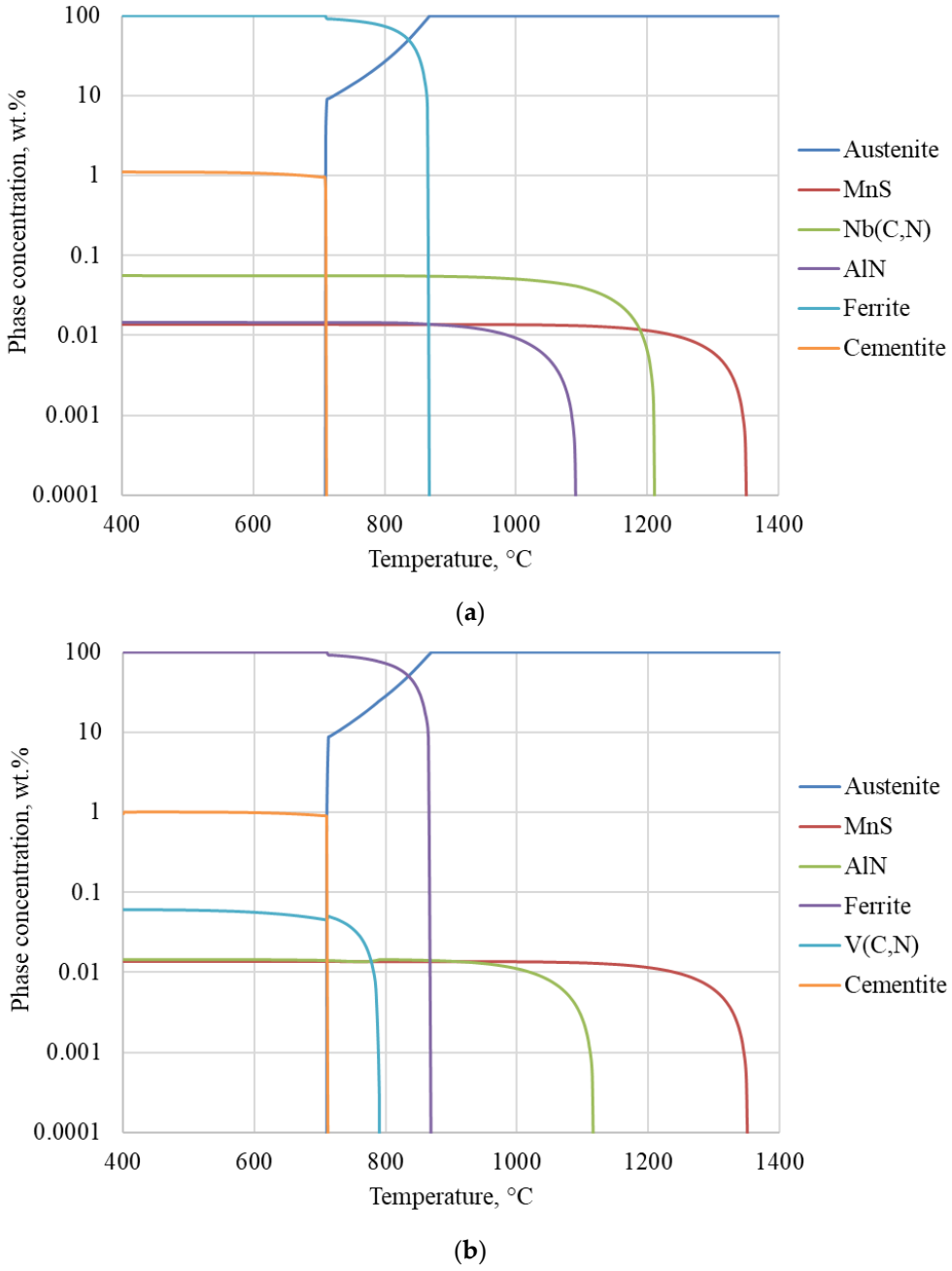

Figure 7. Temperature dependence of the phase composition of model steel containing, wt.%: 0.08 C, 0.60 Mn, 0.10 Si, 0.045 Al, 0.005 S, 0.005 P, 0.005 N and (**a**) 0.05 Nb, (**b**) −0.05 V.

Two steels with various vanadium contents, wt.%: 0.151 C–0.374 Si–1.520 Mn–0.047 Nb–0.020 Ti–0.029 V and 0.156 C–0.370 Si–1.601 Mn–0.047 Nb–0.020 Ti–0.041 V, were studied in [41]. Steel with a high vanadium content (0.041 wt.%) has a deeper trough: the smallest redaction of area is 66.5% at a fracture temperature of 700 °C, while steel with 0.029% V has 75.5%. Figure 8 shows the decrease in the minimum value of RA for steel of the base composition, wt.%: 0.11–0.13 C, 0.3–0.34 Si, 1.39–1.43 Mn, 0.016–0.02 P, 0.003–0.004 S, 0.005–0.0053 N, with increasing concentration V from 0.009 to 0.1 wt.% [42]. The best ductility was in steel with 0.009 wt.% V: the minimum redaction of area was about 53% at 800 °C.

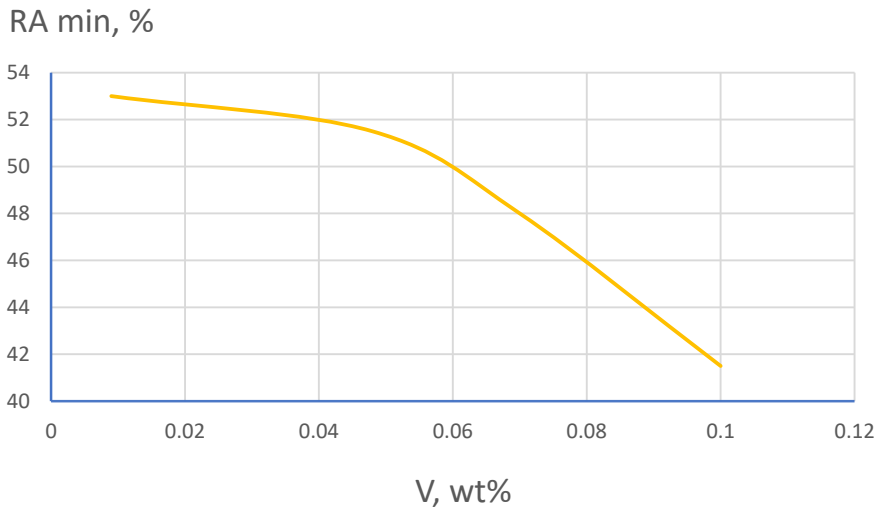

Figure 8. Dependence of the minimum value of hot ductility on vanadium content for steel of basic composition, wt.%: 0.11–0.13 C, 0.3–0.34 Si, 1.39–1.43 Mn, 0.016–0.02 P, 0.003–0.004 S, 0.005–0.0053 N.

It should be noted that the effect of the size of precipitates in low-carbon vanadium microalloyed steels was studied in the works [43,44]. An analysis of the hot ductility loss in [43] showed that small particles (~6 nm) were more harmful than larger ones (~20 nm), since they slowed down dynamic recrystallization more strongly. The results of the study [44] of steel with composition, wt.%: 0.06 C–0.4 Si–1.0 Mn–0.01 P–0.005 S–0.01 Ti—0.07 V–0.2 Cu–0.5 Cr–0.25 Ni, show that hot ductility changes dramatically from 975 up to 825 °C, when the size of the precipitates changes in the range from 10 to 30 nm. The authors explained this by the fact that finer precipitates weakened the grain boundaries and were the sites of nucleation of ferrite films.

In [84], vanadium was found to be a useful additive for Nb-microalloyed with a low nitrogen content, probably because vanadium retards niobium precipitation by increasing Nb(CN) solubility. A positive effect of niobium addition on V-microalloyed steel was also established. Although a small addition of niobium (0.015 wt.%) to steel with 0.05 wt.% C, 0.0065–0.012 wt.% N, and 0.085 wt.% V increased the temperature at which ductility began to deteriorate, in the low-temperature region of austenite (800–900 °C), ductility improved. Studies have shown that this was due to the fact that niobium delays dynamic and post-dynamic NbV(CN) precipitation.

2.7. Effect of Boron Nitride

Since boron can form BN with nitrogen, the presence of these dispersed precipitates adversely affects hot plasticity. Therefore, the influence of boron strongly depends on the rate and cooling conditions, which determines the form of the presence of boron, as well as the size of BN precipitates. Table 4 shows examples of the results of some studies showing the opposite effect of boron, depending on the cooling conditions. Slow cooling promotes boron segregation at the austenite grain boundaries, therefore leading to better ductility.

In 2010, Mintz et al. [34], based on a summary of a large number of works on the study of the hot ductility of steels, identified the following reasons for the favorable effect of boron:

- Since the boron atom is a small atom, it segregates easily at austenite grain boundaries, reducing the boundary slip, which improves creep ductility. In addition, it may take up vacant sites that would otherwise form nucleation sites for fine precipitates, such as Nb(CN) and TiN;
- Boron prevents the formation of ferrite at the austenite grain boundaries causing it to precipitate within the matrix allowing the strain to be accommodated more uniformly;
- Boron causes a coarse precipitation to occur at the boundaries instead of a fine precipitation within the matrix reducing the stress acting on the boundaries.

Table 4. Effect of boron on the hot ductility of low-carbon steels.

	Chemical Composition, wt.%												Effect	Cooling	Ref.
No	**C**	**Si**	**Mn**	**Al**	**Nb**	**Ti**	**Mo**	**S**	**P**	**N**	**B**	**Fe**			
1	0.081	0.139–0.149	0.974–0.983	0.020–0.031	0.02	-	-	0.003	0.010–0.011	0.005–0.006	0.002	Bal.	Positive	1 °C/s	[86]
2	0.05–0.15	0.14–0.23	0.95–1.65	0.02	0.035–0.05	0.02–0.03	0.03, <0.017	0.007–0.008	0.009–0.012	0.0048–0.0092	0.002–0.0043	Bal.	Positive	10 °C/s–heating–cooling	[87,88]
3	0.040–0.048	0.062–0.070	0.495–0.540	0.023–0.028	-	-	0.040–0.041	0.011–0.012	0.015–0.016	0.0048–0.0049	0.0027	Bal.	Positive	1 °C/s	[89]
4													Negative	20 °C/s	
5	0.039–0.043	0.60–0.65	0.495–0.530	0.023–0.027	-	-	0.040–0.041	0.011–0.012	0.015–0.017	0.0011–0.0049	0.0016–0.0026	Bal.	Negative	20 °C/s	[90]
6													Negative	20 °C/s–heating–cooling	
7	0.15–0.17	0.19	1.42–1.44	0.028–0.029	0.024–0.029	0.012–0.014	-	0.018	0.013	0.0060–0.0065	0.0025–0.0045	Bal.	Positive	3 °C/s	[91]
8	0.071	0.1–0.8	1.807–1.936	0.0306–0.0387	0.047–0.048	0.085–0.117	-	0.002–0.003	-	Not specified	0.002–0.0024	Bal.	Positive	1 °C/s to 910 °C–soaking–0.01 °C/s	[92]
9	0.10	0.29–0.32	1.96–1.99	0.023–0.030	0.031	0.0035	-	0.005–0.006	0.005	0.0030–0.0035	0.005–0.01	Bal.	Positive	3 °C/s	[93]
10	0.09	Mn+Si < 2.1		0.03–0.04	Nb+V+Ti < 0.17		0.011–0.016	0.005	-	0.005–0.006	0.003, 0.0002	Bal.	Negative	Natural	[94]
11													Positive	10 °C/s + thermal cycling	

Ductility generally improves with an increasing B/N ratio, and a ratio of 0.8:1 (stoichiometric) has been found to provide the greatest ductility at high cooling rates. While there is a window in which boron additions are beneficial to ductility and can help avoid cracking, it is quite narrow and explains the increased cracking often seen when conditions are not tightly controlled.

In addition, the benefit of adding boron is to prevent the formation of aluminum nitride. Although AlN is much more thermodynamically stable than BN, its precipitation is very slow and on cooling it always forms BN first. Then its effect on hot ductility depends on the particle size. Of the two, AlN is the more harmful. Perhaps this is due to the fact that the nucleation and growth of AlN is much slower, and the dynamic precipitation is usually more dispersed, and AlN precipitation occurs mainly at the boundaries.

The results of [86] show that adding 0.002 wt.% B to 0.08 C–1.0 Mn–0.02 Nb steel greatly improves hot ductility at a cooling rate of 1 °C/s. RA values were >90% over the entire temperature range of 700–850 °C. Large $Fe_{23}(BC)_6$ particles were found at the boundaries and in the matrix. Another possibility that boron addition leads to an increase in the ductility of steels containing niobium is that these coarse $Fe_{23}(BC)_6$ particles contain a significant amount of nitrogen, which should reduce the amount of N and C available for the precipitation of fine Nb(CN) precipitates during deformation.

More recent works have focused on studying the effect of co-microalloying with boron and titanium [91–96]. In the experiments, a cooling rate of 3 °C/s was used. This combination has been shown to be highly effective. This was due to the inhibition of the formation of intergranular ferrite by the segregation of dissolved boron at the grain boundary, since titanium prevented the binding of boron to nitride due to the formation of TiN. Moreover, the addition of Ti reduces the amount of AlN and NbN [95,96]. It should be noted that, with an increase in the strain rate from 10^{-4} to 10^{-2} s^{-1}, a decrease in the amount of BN and TiN precipitates and an increase in their size was observed, which was accompanied by an improvement in hot ductility [96].

In a study [93] for steel with base composition No. 9 indicated in Table 4, the best results were obtained at 58–100 ppm B and 35 ppm Ti. The value of the reduction in area in the temperature range of 800–1250 °C was 80–50%. The authors also noted that the hot ductility of the steel was favorably affected by iron boride Fe_2B, which precipitated along the boundaries of austenite grains.

The authors of [94] suggested that the positive effect of boron during the joint microalloying of steel with boron, niobium, and titanium results in the modification and refinement of the initial austenite grain.

3. Effect of Excess Phases on the Homogeneity of Composition and Microstructure

The problem of increasing the homogeneity of the composition, structure, and properties of metal in modern metallurgical technologies is one of the most important, since it largely controls the properties and quality of steel. It applies to all stages of the metal, from smelting to the production of finished metal products [20,21,32,33,97–99]. For example, in [100], based on the testing of samples taken from four places within the product, i.e., front-centre, back-centre, centre-centre and centre-edge, it was shown that there was at least 10% variation in mechanical properties within one roll. This phenomenon is directly related to modern steel production technology and the phenomena and transformations that occur. In the smelting and ladle processing of liquid steel, this problem is mainly solved by using treatment of the melt with an inert gas. The main contribution to the formation of chemical and structural inhomogeneity is made by segregation processes during steel crystallization. Despite the use of special technological methods of soft reduction, electromagnetic mixing, introduction of macrocoolers into the axial zone of a continuously cast billet, etc., it is not possible to completely prevent the development of segregation processes. It is known that the formation of certain types, including glassy non-metallic inclusions at the final stages of ladle processing during the continuous casting of steel, leads to a significant inhibition

of heat and mass transfer processes and, accordingly, the development of segregation processes during steel crystallization [101–103].

It is known that the steel is in a non-equilibrium state. The formation of dispersed precipitates of excess phases, which improve the properties of steel, increases the degree of non-equilibrium of its state due to an increase in surface energy. This review aimed specifically to establish the role of the precipitation of excess phases formed during the processing of solid steel on the indicators of the homogeneity of the composition and structure of rolled products. The high importance of obtaining a homogeneous composition and structure of rolled products was due to a significant improvement in the indicators of its properties and quality. In particular, for steel composition, wt.% 0.098 C–0.305 Si–1.28 Mn–0.033 Al–0.019 Ti–0.070 Nb–0.0068 N, the relative elongation during the formation of an inhomogeneous microstructure decreased from 27% to 20% [32].

Chemical and structural inhomogeneity is also formed in the process of hot rolling due to uneven cooling of the rolled product along its thickness. According to the estimates made in [99], when studying rolled products with a thickness of 80 mm, the cooling rate in the surface layer was 7–15 °C/s, at 1/4 of the thickness—1–3 °C/s, and in the central part—1 °C/s. In many respects, the heterogeneity of the composition and structure of the metal was due to the precipitation of carbonitride phases. For the steel of a given chemical composition, the equilibrium temperatures at the beginning of the formation of carbonitrides were first reached in the surface layers, which cool faster than the areas remote from the surface. Herewith, in the areas adjacent to the surface, carbonitride precipitates began to form and a concentration gradient of carbon and microalloying elements in the solid solution increased along the thickness of the rolled product—their content (chemical potential) in the solid solution in the near-surface layers became lower than in the axial zone. This led to the intense diffusion of carbon and other elements from the axial zone to the surface, as a result of which the content of these elements in the steel (primarily carbon, due to its greater diffusion mobility) became inhomogeneous over the thickness of the rolled product. Such inhomogeneity of the chemical composition also leads to structural inhomogeneity in the thickness of rolled products. At the same time, due to the formation of different amounts of carbonitride precipitates of microalloying elements in various zones along the thickness of the rolled products, a significant difference also occurred in the dispersion of the microstructure over the cross-section of the rolled products.

In the work [98], sheet steel with the composition, wt.%: 0.15 C–0.98 Mn–0.28 Si–0.02 Al–0.08 Ti–0.0027 N with a thickness of 40 mm was studied. It was found that the near-surface layer and the mid-thickness region differed both in grain size and in the size of titanium carbide precipitates. The grain sizes were 13.2 and 18.6 μm, respectively. The TiC precipitates were 5–20 nm in size near the surface, and larger in the region of the middle thickness of the precipitates: 10–30 nm. This was the reason for the difference in mechanical properties. The strength and hardness in the surface layer was higher and the ductility was lower. The yield strength, tensile strength, and elongation differed by 50 MPa, 37 Mpa, and 7.2%, respectively. To improve the homogeneity, the authors used the thermos-deformation treatment mode with a higher cooling rate.

As a result of the study [21], a correlation was established between the uniformity of the microstructure and the toughness of the steel with composition, wt.%: 0.05 C–1.6 Mn–0.06 Si–0.029 Nb–0.01 Mo–0.028 Al–0.005 N. It has been shown that, as the coiling temperature is lowered, the toughness improves. The best performance was obtained at 450 °C.

In the study of high-strength low-alloyed steels of various microalloying systems in [32,33], it was shown that the uniformity of the composition and microstructure can be significantly influenced by changing the temperature of the beginning of hot rolling in the finishing group of stands, T_{bf}, which leads to a change in the intensity of mass transfer processes and formation of carbide, carbonitride precipitates. As a result, the chemical structural inhomogeneity of the metal formed at the stage of continuous casting of billets can be largely eliminated during hot rolling.

It was found in [32,33] that, for low-carbon Nb, Nb-Ti, Nb-V microalloying steels, similar regularities are observed (Table 5). At low values of T_{bf}, the concentration of carbon detected near the surface is equal to or even somewhat lower than its content in the axial zone of the rolled product. An increase in T_{bf} leads to the formation of surface layers much more enriched in carbon compared to the axial zone of the rolled product. Despite the closeness of the established regularities, the mechanisms of this phenomenon are different depending on the microalloying system.

Table 5. Chemical homogeneity (carbon content) in steels of various microalloying systems according to [33].

The Content of Microalloying, wt.%	T_{bf}, °C	Carbon Content, across the Cross-Section of Rolled Products, wt.%	
		Surface	Axial Zone
0.073 Nb	960	0.087	0.090
	990	0.088	0.089
	1030	0.092	0.086
0.071 Nb–0.018 Ti	950	0.084	0.085
	990	0.088	0.083
	1040	0.089	0.082
0.064 Nb–0.057 V	970	0.089	0.091
	1000	0.090	0.091
	1030	0.093	0.089

3.1. Influence of Precipitation in Nb-Microalloyed Steels

Figure 9 shows the result of calculating the equilibrium composition of steel with composition, wt.%: 0.088 C–1.44 Mn–0.39 Si–0.034 Al–0.073 Nb–0.007 N. The concentration of MnS precipitates changes little with temperature. With a decrease in temperature, in the range of hot rolling, a region of stability of niobium carbonitride precipitates first appears, and then aluminum nitride. Since the AlN formation is kinetically hindered and requires a high degree of supersaturation of the solid solution with aluminum and nitride, it may not occur during hot rolling due to the competitive formation of Nb(CN) precipitates. In the range of low temperatures of ferrite stability, the formation of cementite and carbide of complex composition Me_7C_3 is possible. Thus, the main phase that precipitates during hot rolling is niobium carbonitride. Its precipitation begins at a temperature of about 1250 °C. Consequently, by the beginning of rolling in the finishing group of stands T_{bf} = 950–1050 °C, in the case of thermodynamic equilibrium, its predominant fraction should precipitate. Therefore, at high values of T_{bf} = 1020–1050 °C, there is already a sufficiently high thermodynamic stimulus for its formation, and at the same time, a high diffusion mobility of atoms of the phase-forming components, primarily carbon and nitrogen, is maintained. As a result of redistribution, the surface layers of rolled products are enriched in carbon and other elements. However, due to kinetic and time constraints, the state of thermodynamic equilibrium was not reached. Therefore, the actual amount of Nb(CN) precipitates formed is less than it follows from the data in Figure 9.

Accelerated cooling of the metal, in the case of lower values of T_{bf} = 950–980 °C, led to a decrease in the number of Nb(CN) precipitates that were able to form and, accordingly, the stimulus for the diffusion redistribution of carbon and other steel components. In addition, a lower temperature corresponded to a lower diffusion mobility of atoms. In accordance with the above points, a decrease in Tbf led to a decrease in the intensity of carbon redistribution to the surface of the rolled product. As a result, its concentration observed at the surface of the rolled product corresponded to or was even slightly lower than in the axial zone of the rolled product (Table 5).

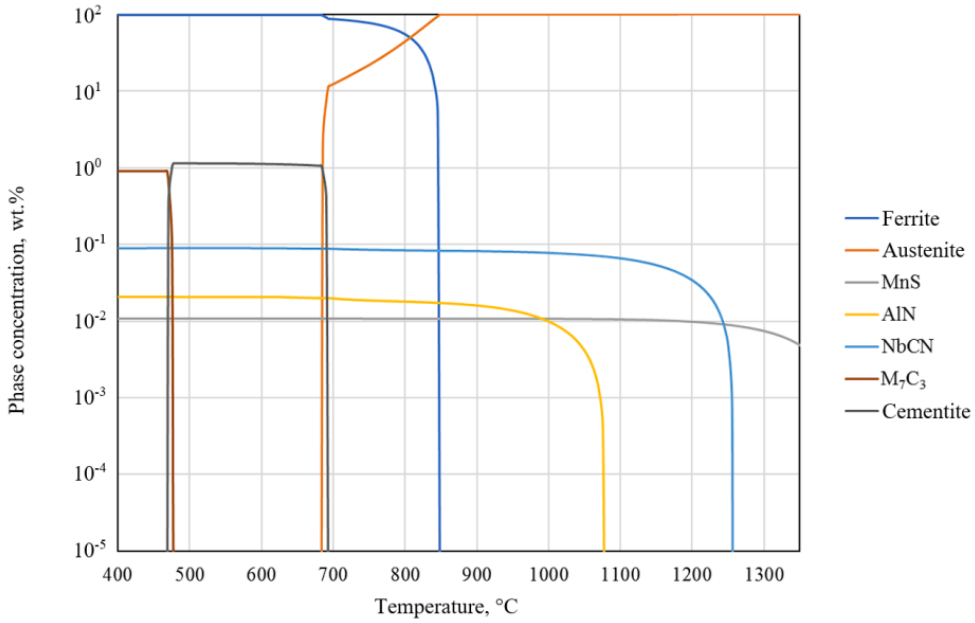

Figure 9. Temperature dependence of the phase composition of steel containing, wt.%: 0.088 C–1.44 Mn–0.39 Si–0.034 Al–0.073 Nb–0.007 N. Reprinted with permission from ref. [33]. Copyright 2023 Metallurgizdat.

It should be noted that the key goal of microalloying steel with niobium is aimed at restraining recrystallization during rolling in order to obtain a more dispersed microstructure. This occurs both due to the niobium present in the solid solution due to diffusion deceleration, and due to Nb(CN) precipitates blocking the movement of grain boundaries. The intensity of the formation of Nb(CN) precipitates increases significantly when deformation is applied [77]. For these reasons, a decrease in T_{bf} is a favorable factor for obtaining a more finely dispersed uniform microstructure. Indeed, the retention of a higher concentration of niobium in the solid solution and the presence of a larger amount of dispersed Nb(CN) precipitates more effectively restrain recrystallization during rolling in the finishing group of stands and, as a result, refine the grain structure.

In accordance with the abovementioned points, at low values of T_{bf}, a uniform fine-grained structure of rolled products is observed both at the surface and in the axial zone of the rolled product, and at high values of T_{bf}, a pronounced grain size inhomogeneity of rolled products is observed near the surface and in the axial zone [32,33]. This is clearly seen in the optical micrographs (Figure 10). The average grain size when using T_{bf} = 950 °C in the axial and surface zones is 3–5 μm (Figure 10a,b). The appearance of grain size inhomogeneity (Figure 10c,d), as is known, first of all leads to a decrease in ductility. Relative elongation at low values of T_{bf} = 950 °C is 24%, at T_{bf} = 1020 °C it is 22% [32].

The results obtained are explained by the predominant formation of Nb(CN) precipitates in the near-surface zone of rolled products, which leads to more efficient grain refinement. Due to the significant redistribution of carbon and, to some extent, niobium, the content of Nb(CN) precipitates in the axial zone of the rolled product is significantly less and the grain size is larger.

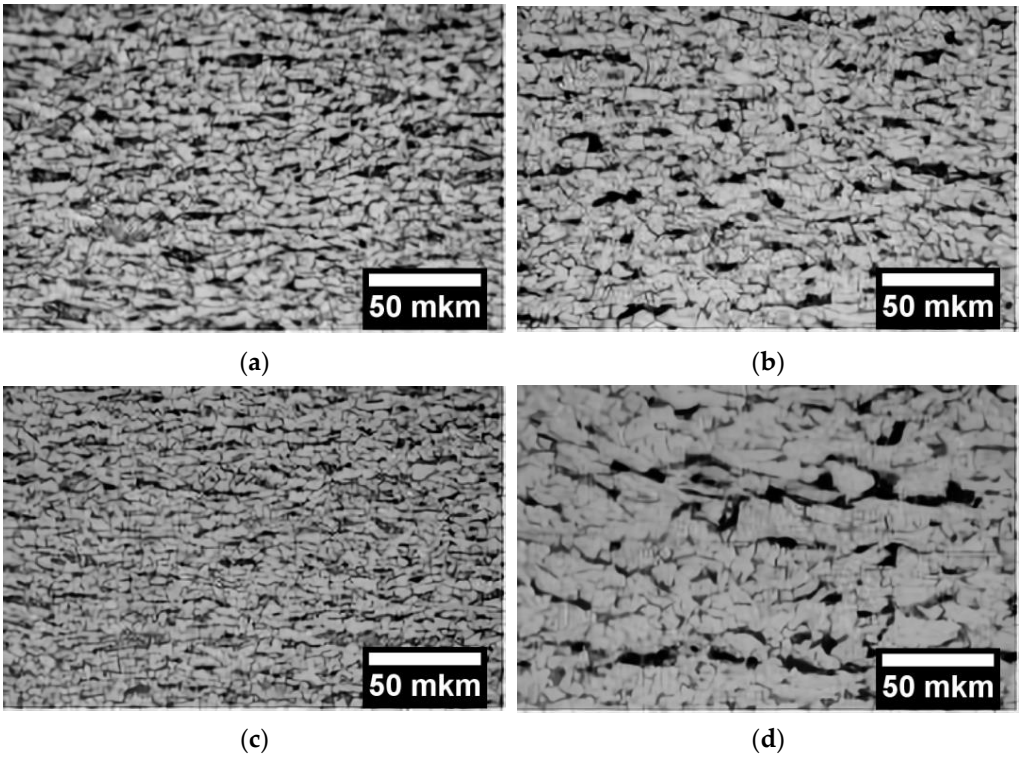

Figure 10. Ferrite–pearlite microstructure of steel with composition, wt.%: 0.121 C–0.394 Si–1.63 Mn–0.039 Al–0.0079 N–0.054 Nb: (**a**) at T_{bf} = 950 °C on the surface, (**b**) at T_{bf} = 950 °C in the axial zone, (**c**) at T_{bf} = 1020 °C on the surface, (**d**) at T_{bf} = 1020 °C in the axial zone. ×500 Reprinted with permission from ref. [32]. Copyright 2023 Metallurgizdat.

3.2. Influence of Precipitation in Nb-Ti and Nb-V Microalloyed Steels

Figure 11 shows the results of calculating the equilibrium composition of steels microalloyed together with Nb-Ti or Nb-V. Just as in the case of microalloying only with niobium, the concentration of MnS precipitates changes little with temperature. In Nb-Ti steel (Figure 11a), at high temperatures, titanium is almost completely bound to TiN nitride, the content of which remains unchanged with a decreasing temperature. The formation of AlN precipitates does not occur due to the almost complete binding of nitrogen by the titanium present in steel. In the range of low temperatures of ferrite stability, the formation of cementite and carbide of complex composition Me_7C_3 is possible.

In Nb-Ti microalloyed steel, due to the presence of titanium, precipitates of almost individual NbC carbides are formed. It is well known that a decrease in the nitrogen content in Nb(CN) increases its effectiveness on restraining recrystallization, apparently due to kinetically more favorable conditions for the formation of carbide rather than carbonitride of niobium. As a result, this leads to a more intense formation of carbide precipitates at high T_{bf} and the most significant redistribution of carbon from the axial zone to the surface of the rolled product is observed (Table 5). However, rolled steel of the considered composition contains the largest amount of carbide precipitates, which lead to the most effective refinement of the grain structure. Interrelated is the fact that, in order to obtain a structure uniform in the cross-section of the rolled product for steel of this composition, the most significant decrease in T_{bf} is necessary.

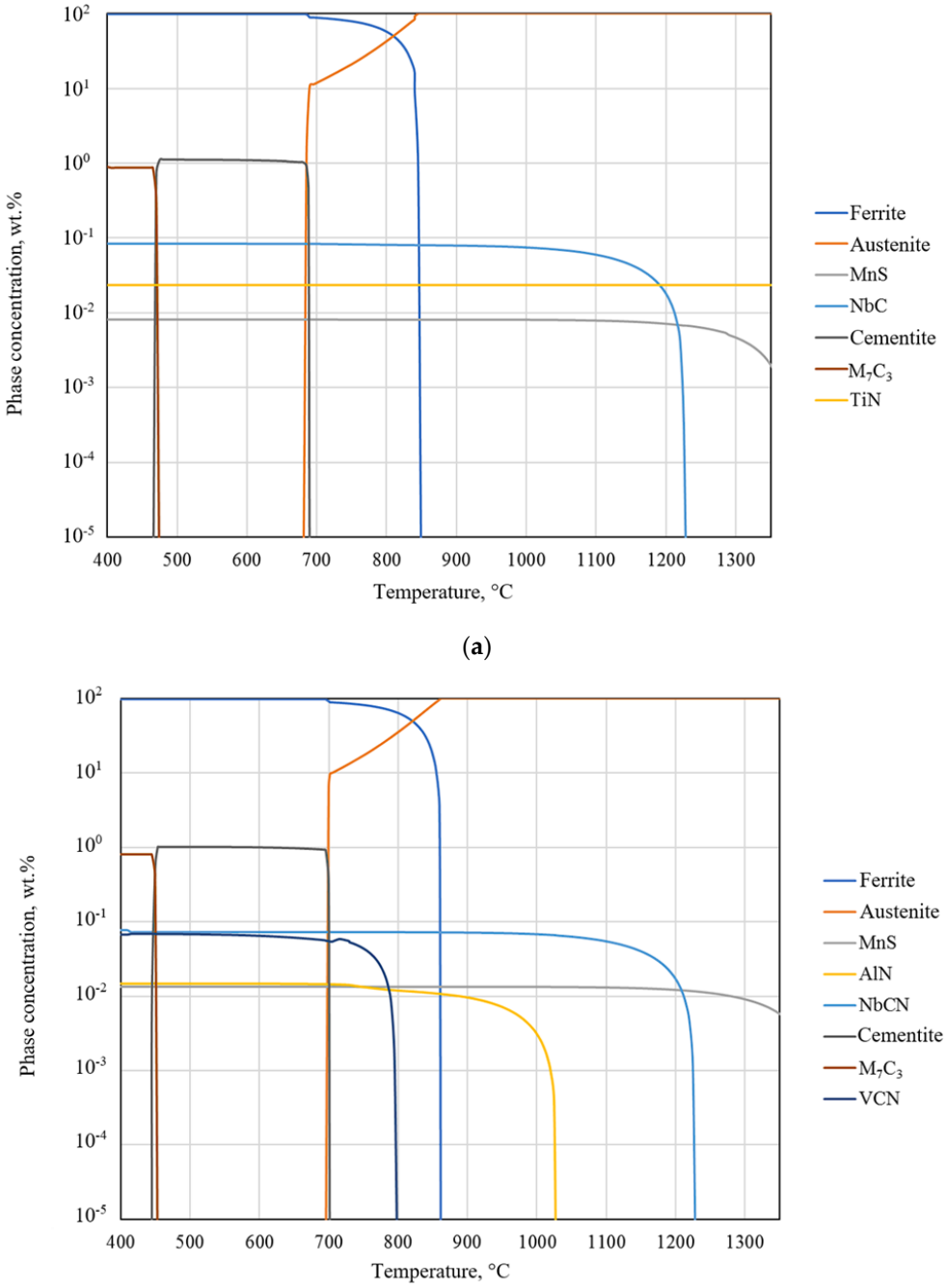

Figure 11. Temperature dependence of the phase composition of steel containing, wt.%: (**a**) 0.085 C–1.40 Mn–0.35 Si–0.038 Al–0.071 Nb–0.018 Ti–0.005 N, (**b**) 0.091 C–1.09 Mn–0.34 Si–0.029 Al–0.064 Nb–0.057 V–0.005 N [33].

To a lesser extent, formulated tendencies were observed in Nb-V microalloyed steel rolled products. Due to low formation temperatures (Figure 11b), V(CN) precipitates provided a much smaller contribution to the formation of structure inhomogeneity. Therefore, the degree of chemical heterogeneity was mainly due to the intensity of the formation of niobium carbonitride.

3.3. Influence of Precipitation in Mo-Microalloyed Steels

Studies of the effect of molybdenum additions to Nb-microalloyed steels [20,21] have shown that molybdenum can lead to a deterioration in the uniformity of the microstructure

due to the formation of martensite–austenite islands. Similar results were obtained for steels additionally microalloyed with boron [20]. At the same time, it is known that molybdenum significantly accelerates the nucleation and inhibits the growth of carbonitride precipitates [104]. Therefore, an increase in the intensity of the nucleation of precipitates will contribute to the redistribution of carbon and, as a result, an increase in heterogeneity. This was observed when adding molybdenum to Nb-V microalloyed steel [33].

The results of the study of rolled products from Ti-Mo microalloyed steel [33] showed patterns, which were opposite for the features of carbon redistribution and structure formation in Nb, Nb-Ti, Nb-V steels. The inhomogeneous composition and structure of rolled products occurs at low values of T_{bf}. Its increase leads to an improvement in the indicators of chemical and structural homogeneity (Figure 12) [33].

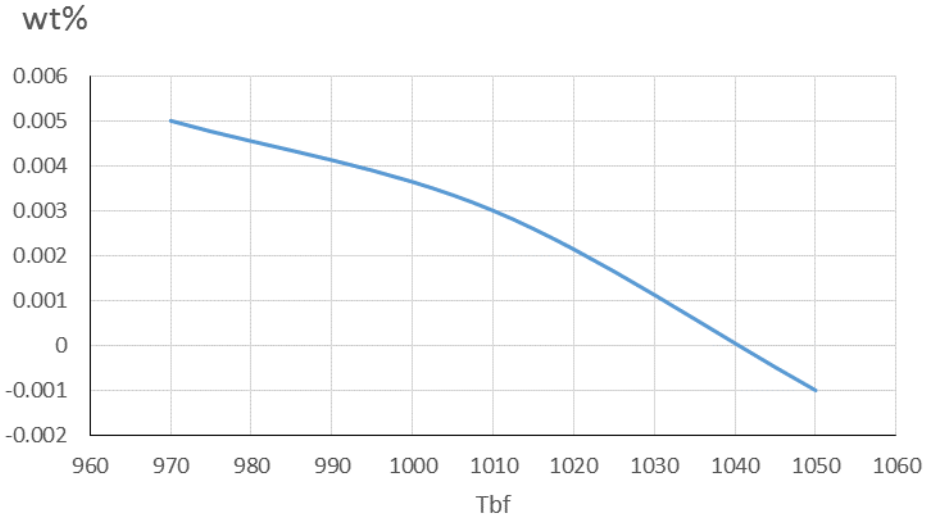

Figure 12. Dependence of the difference between the carbon content in the surface layer and the axial zone in rolled products on the temperature at the beginning of finishing rolling for steel, wt.%: 0.061 C–0.07 Si–1.57 Mn–0.045 Al–0.005 N–0.092 Ti–0.20 Mo.

The noted feature was due to the specific kinetics of the formation of TiC precipitates. The formation of these precipitates in austenite was kinetically difficult and occurred at a significant rate only at relatively low temperatures of about 850 °C [105]. As a result, at T_{bf} = 950 °C, their formation and, accordingly, the redistribution of carbon from the axial zone of rolled products with the formation of a heterogeneous composition, structure, and reduced properties of rolled products were characterized by the greatest intensity. At higher temperatures, the formation of TiC precipitates is kinetically hindered and prevents the possibility of a reverse redistribution of carbon, which controls the change in the structure and properties of rolled products.

4. Conclusions

The study and analysis of the effect of precipitation of excess phases on hot ductility, homogeneity of composition, and structure of high-strength low-alloy steels made it possible to establish the following regularities.

- Sulfide precipitates reduce hot ductility due to the formation of an FeS liquid layer along the grain boundaries and the appearance of microcavities (PFZs) around small precipitates of (Fe,Mn)S and MnS. To improve hot ductility, it is advisable to reduce the sulfur content and increase the concentration of manganese in order to achieve favorable forms of the presence of sulfur.
- Precipitation of niobium carbonitride adversely affects hot ductility by facilitating the joining of cracks at large precipitate sizes and the formation of precipitate-free zones at a small size. This effect is enhanced with an increase in the nitrogen content in the steel.

- Under conditions close to production, the formation at a high temperature of TiN precipitates of large sizes capable of serving as a substrate for the subsequent deposition of niobium carbonitride is a factor that improves hot ductility. An additional positive factor is the prevention of the formation of unfavorable precipitates of AlN, BN.
- The negative effect of AIN precipitates is realized by two mechanisms: sliding along the grain boundaries as a result of their precipitates and microvoid coalescence in ferrite. In steels microalloyed with Nb, the precipitation of AIN inhibits the formation of Nb(CN) precipitates, which leads to their smaller size. The deterioration of the hot ductility value is also possible due to MnS/AlN co-precipitation on dislocations occurring after rapid cooling and reheating.
- The negative effect of V(CN) precipitates on hot ductility is similar to Nb(CN) and increases with increasing nitrogen content in steel.
- At high cooling rates, the stoichiometric ratio B/N = 0.8:1 obtained in BN precipitates provides the highest steel ductility, including by preventing the formation of AlN, Nb(CN).
- The chemical and structural inhomogeneity of high-strength low-alloy steels formed at the stage of continuous casting of billets can be largely eliminated during hot rolling by controlling the formation of carbide (carbonitride) precipitates of microalloying elements. The most intense redistribution of carbon from the axial zone to the surface of the rolled product occurs in Nb-Ti microalloyed steels due to the more effective action of NbC precipitates and requires the greatest reduction in T_{bf}.
- The formation of Nb(CN) precipitates in Nb-microalloyed steel is kinetically more complicated, and their effect on structure formation is less effective. Therefore, there is less intensive carbon redistribution and structure change, which allows the use of higher T_{bf}.
- With complex Nb-V microalloying, only Nb exhibits the effect of action. The presence of Mo in the composition of steel accelerates the nucleation, but inhibits the growth of carbide (carbonitride) precipitates, which leads to the intensification of carbon redistribution processes and, accordingly, changes in the structure of rolled products.
- For Ti-Mo microalloyed steel, the features opposite to those presented above are characteristic of the redistribution of carbon, the formation of structure and properties, depending on T_{bf}. An inhomogeneous composition and structure occur at low values of T_{bf}. Its increase leads to an improvement in the chemical and structural homogeneity of steel. This is due to the specific kinetics of TiC formation, which proceeds most intensively at relatively low temperatures.

Author Contributions: Conceptualization, A.Z.; software, A.K.; thermodynamic calculation, A.K.; writing—original draft preparation, N.A.; writing—review and editing, A.Z. and N.A.; visualization, A.K.; supervision, A.Z.; project administration, A.Z. All authors have read and agreed to the published version of the manuscript.

Funding: This research received no external funding.

Conflicts of Interest: The authors declare no conflict of interest.

References

1. Villalobos, J.C.; Del-Pozo, A.; Campillo, B.; Mayen, J.; Serna, S. Microalloyed steels through history until 2018: Review of chemical composition, processing and hydrogen service. *Metals* **2018**, *8*, 351. [CrossRef]
2. Kong, H.J.; Liu, C.T. A review on nano-scale precipitation in steels. *Technologies* **2018**, *6*, 36. [CrossRef]
3. DeArdo, A.J.; Hua, M.J.; Cho, K.G.; Garcia, C.I. On strength of microalloyed steels: An interpretive review. *Mater. Sci. Technol.* **2009**, *25*, 1074–1082. [CrossRef]
4. Baker, T.N. Titanium microalloyed steels. *Ironmak. Steelmak.* **2019**, *46*, 1–55. [CrossRef]
5. DeArdo, A.J. Niobium in modern steels. *Int. Mater. Rev.* **2003**, *48*, 371–402. [CrossRef]
6. Sun, L.Y.; Liu, X.; Xu, X.; Lei, S.W.; Li, H.G.; Zhai, Q.J. Review on niobium application in microalloyed steel. *J. Iron Steel Res. Int.* **2022**, *29*, 1513–1525. [CrossRef]
7. Lagneborg, R.; Siwecki, T.; Zajac, S.; Hutchinson, B. The role of vanadium in microalloyed steels. *Scand. J. Metall.* **1999**, *28*, 1–86.

8. Zaitsev, A.; Arutyunyan, N. Low-carbon Ti-Mo microalloyed hot rolled steels: Special features of the formation of the structural state and mechanical properties. *Metals* **2021**, *11*, 1584. [CrossRef]
9. Zaitsev, A.; Koldaev, A.; Arutyunyan, N.; Dunaev, S.; D'yakonov, D. Effect of the chemical composition on the structural state and mechanical properties of complex microalloyed steels of the ferritic class. *Processes* **2020**, *8*, 646. [CrossRef]
10. Singh, N.; Casillas, G.; Wexler, D.; Killmore, C.; Pereloma, E. Application of advanced experimental techniques to elucidate the strengthening mechanisms operating in microalloyed ferritic steels with interphase precipitation. *Acta Mater.* **2020**, *201*, 386–402. [CrossRef]
11. Xiong, Z.; Timokhina, I.; Pereloma, E. Clustering, nano-scale precipitation and strengthening of steels. *Prog. Mater. Sci.* **2021**, *118*, 100764. [CrossRef]
12. Larzabal, G.; Isasti, N.; Rodriguez-Ibabe, J.M.; Uranga, P. Evaluating strengthening and impact toughness mechanisms for ferritic and bainitic microstructures in Nb, Nb-Mo and Ti-Mo microalloyed steels. *Metals* **2017**, *7*, 65. [CrossRef]
13. Huang, Y.; Chen, H.; Zhao, Q.; Zhang, S.; Li, X. Influence of nanosized precipitate on the corrosion behavior of high-strength low-alloy steels: A review. *Chin. J. Eng.* **2021**, *43*, 321–331. [CrossRef]
14. Ma, M.T.; Li, K.J.; Si, Y.; Cao, P.J.; Lu, H.Z.; Guo, A.M.; Wang, G.D. Hydrogen embrittlement of advanced high-strength steel for automobile application: A review. *Acta Metall. Sin. Engl. Lett.* **2023**, 1–15. [CrossRef]
15. Fan, E.; Zhang, S.; Xie, D.; Zhao, Q.; Li, X.; Huang, Y. Effect of nanosized NbC precipitates on hydrogen-induced cracking of high-strength low-alloy steel. *Int. J. Miner. Metall. Mater.* **2021**, *28*, 249–256. [CrossRef]
16. Yen, C.N.; Chang, L.W.; Hsu, C.A.; Yang, J.R.; Chang, H.Y.; Wang, S.H.; Chen, H.R. Microstructural variation in fatigued interphase arrayed nano-precipitated Ti-microalloyed steel. *J. Mater. Res. Technol.* **2021**, *15*, 2393–2404. [CrossRef]
17. Majumdar, S.; Gandhi, A.D.; Bisht, M.S. Low cycle fatigue behaviour of a ferritic steel strengthened with nano-meter sized precipitates. >*Mater. Sci. Eng. A* **2019**, *756*, 198–212. [CrossRef]
18. Liu, B.; Hui, W.; Xie, Z.; Zhang, Y.; Zhao, X. Effect of vanadium on fatigue performance of a bainitic forging steel. *Int. J. Fatigue* **2023**, *167 Pt B*, 107398. [CrossRef]
19. Ghosh, S.; Mula, S.; Malakar, A.; Somani, M.; Kömi, J. High cycle fatigue performance, crack growth and failure mechanisms of an ultrafine-grained Nb + Ti stabilized, low-C microalloyed steel processed by multiphase controlled rolling and forging. *Mater. Sci. Eng. A* **2021**, *825*, 141883. [CrossRef]
20. Zurutuza, I.; Isasti, N.; Detemple, E.; Schwinn, V.; Mohrbacher, H.; Uranga, P. Toughness property control by Nb and Mo additions in high-strength quenched and tempered boron steels. *Metals* **2021**, *11*, 95. [CrossRef]
21. Isasti, N.; Jorge-Badiola, D.; Taheri, M.L.; Uranga, P. Microstructural features controlling mechanical properties in Nb-Mo microalloyed steels. *Part II Impact toughness Metall. Mater. Trans. A* **2014**, *45*, 4972–4982. [CrossRef]
22. Sun, M.; Xu, Y.; Du, W. Influence of coiling temperature on microstructure, precipitation behaviors and mechanical properties of a low carbon Ti micro-alloyed steel. *Metals* **2020**, *10*, 1173. [CrossRef]
23. Bu, F.Z.; Wang, X.M.; Yang, S.W.; Shang, C.J.; Misra, R.D.K. Contribution of interphase precipitation on yield strength in thermomechanically simulated Ti–Nb and Ti–Nb–Mo microalloyed steels. *Mater. Sci. Eng. A* **2015**, *620*, 22–29. [CrossRef]
24. Xu, L.; Wu, H.; Tang, Q. Effects of Coiling Temperature on microstructure and precipitation behavior in Nb–Ti microalloyed. *ISIJ Int.* **2018**, *58*, 1086–1093. [CrossRef]
25. Sesma, L.G.; Lopez, B.; Pereda, B. Effect of deformation sequence and coiling conditions on precipitation strengthening in high Ti–Nb-microalloyed steels. *Metall. Mater. Trans. A* **2022**, *53*, 2270–2285. [CrossRef]
26. Chen, J.; Lv, M.; Tang, S.; Liu, Z.; Wang, G. Influence of cooling paths on microstructural characteristics and precipitation behaviors in a low carbon V-Ti microalloyed steel. *Mater. Sci. Eng. A* **2014**, *594*, 389–393. [CrossRef]
27. Hu, C.Y.; Dong, H.Y.; Wu, G.H.; Wu, K.M.; Misra, R.D.K. A Thermodynamic analysis of strengthening mechanisms and process-structure-property relationships in Ti-Nb-Mo high-strength ferritic alloy. *J. Mater. Eng. Perform.* **2021**, *30*, 2946–2954. [CrossRef]
28. Rodionova, I.; Amezhnov, A.; Alekseeva, E.; Gladchenkova, Y.; Vasechkina, I. Effect of carbonitride precipitates on the corrosion resistance of low-alloy steels under operating conditions of oil-field pipelines. *Metals* **2021**, *11*, 766. [CrossRef]
29. Rodionova, I.; Arutyunyan, N.; Amezhnov, A.; D'yakonov, D.; Gladchenkova, Y.; Dunaev, S.; Vasechkina, I. Effect of nanosized precipitates on corrosion resistance of Nb-microalloyed steels. *Metals* **2022**, *12*, 636. [CrossRef]
30. Fan, E.; Zhao, Q.; Chen, H.; Ma, Y.; Hai, C.; Yang, Y.; Huang, Y.; Li, X. Effects of Nb on stress corrosion cracking of various heat-affected zone microstructures of E690 steel under cathodic potential. *J. Mater. Eng. Perform.* **2023**, 1–20. [CrossRef]
31. Davis, C.L.; Strangwood, M. Preliminary study of the inhomogeneous precipitate distributions in Nb-microalloyed plate steels. *J. Mater. Sci.* **2002**, *37*, 1083–1090. [CrossRef]
32. Zaitsev, A.I.; Koldaev, A.V.; Karamysheva, N.A.; Rodionova, I.G. Mechanisms for improving chemical and structural homogeneity of hot-rolled product for objects prepared by hot stamping. *Metallurgist* **2016**, *59*, 1086–1095. [CrossRef]
33. Zaitsev, A.I.; Rodionova, I.G.; Koldaev, A.V.; Arutyunyan, N.A.; Dunaev, S.F. Study of conditions for improving chemical and structural homogeneity of ferritic class hot-rolled steels. *Metallurgist* **2021**, *64*, 997–1007. [CrossRef]
34. Mintz, B.; Crowther, D.N. Hot ductility of steels and its relationship to the problem of transverse cracking in continuous casting. *Int. Mater. Rev.* **2010**, *55*, 168–196. [CrossRef]
35. Mintz, B.; Qaban, A.; Kang, S.E. The influence of small additions of alloying elements on the hot ductility of AHSS steels: A critical review: Part 2. *Metals* **2023**, *13*, 406. [CrossRef]

36. Banks, K.M.; Tuling, A.; Mintz, B. The influence of N on hot ductility of V-, Nb-, and Nb-Ti- containing steels using improved thermal simulation of continuous casting. *J. S. Afr. Inst. Min. Metall.* **2011**, *111*, 711–716. Available online: http://www.scielo.org.za/scielo.php?script=sci_arttext&pid=S2225-62532011001000010 (accessed on 1 February 2023).
37. Banks, K.M.; Tuling, A.; Klinkenberg, C.; Mintz, B. Influence of Ti on hot ductility of Nb containing HSLA steels. *Mater. Sci. Technol.* **2011**, *27*, 537–545. [CrossRef]
38. Commineli, O.; Abushosa, R.; Mintz, B. Influence of titanium and nitrogen on hot ductility of C-Mn-Nb-Al steels. *Mater. Sci. Technol.* **1999**, *15*, 1058–1068. [CrossRef]
39. Zhang, M.; Li, H.; Gan, B.; Huang, C.; Li, H.; Zhong, Y.; Li, L. Effects of micro-Ti addition on improving hot ductility of Nb-bearing ultra high strength steels. In *Frontiers in Materials Processing, Applications, Research and Technology*; Muruganant, M., Chirazi, A., Raj, B., Eds.; Springer: Singapore, 2018; pp. 277–285. [CrossRef]
40. Abushosha, R.; Vipond, R.; Mintz, B. Influence of sulphur and niobium on hot ductility of as cast steels. *Mater. Sci. Technol.* **1991**, *7*, 1101–1107. [CrossRef]
41. Song, S.; Tian, J.; Xiao, J.; Fan, L.; Yang, Y.; Yuan, Q.; Gan, X.; Xu, G. Effect of vanadium and strain rate on hot ductility of low carbon microalloyed steels. *Metals* **2022**, *12*, 14. [CrossRef]
42. Mohamed, Z. Hot ductility behavior of vanadium containing steels. *Mater. Sci. Eng. A* **2002**, *326*, 255–260. [CrossRef]
43. Banks, K.; Koursaris, A.; Verdoorn, F.F.; Tuling, A. Precipitation and hot ductility of low C-V and low C-V-Nb microalloyed steels during thin slab casting. *Mater. Sci. Technol.* **2001**, *17*, 1596–1604. [CrossRef]
44. Sun, Y.H.; Zeng, Y.N.; Cai, K.K. Hot ductility of Ti-V bearing microalloyed steel in continuous casting. *J. Iron Steel Res. Int.* **2014**, *21*, 451–458. [CrossRef]
45. Mintz, B.; Yue, S.; Jonas, J.J. Hot ductility of steels and its relationship to the problem of transverse cracking during continuous casting. *Int. Mater. Rev.* **1991**, *36*, 187–220. [CrossRef]
46. Mintz, B. The Influence of composition on the hot ductility of steels and to the problem of transverse cracking. *ISIJ Int.* **1999**, *39*, 833–855. [CrossRef]
47. Mintz, B.; Qaban, A. The influence of precipitation, high levels of Al, Si, P and a small B addition on the hot ductility of TWIP and TRIP assisted steels: A critical review. *Metals* **2022**, *12*, 502. [CrossRef]
48. Shaposhnikov, N.G.; Rodionova, I.G.; Pavlov, A.A. Thermodynamic development of austenite-martensite class corrosion-resistant steels intended for a bimetal cladding layer. *Metallurgist* **2015**, *59*, 1195–1200. [CrossRef]
49. Hillert, M.; Staffanson, L.I. The regular solution model for stoichiometric phases and ionic melts. *Acta Chem. Scand.* **1970**, *24*, 3618–3626. [CrossRef]
50. Sundman, B.; Agren, J. A regular solution model for phases with several components and sublattices, suitable for computer applications. *J. Phys. Chem. Solids* **1981**, *42*, 297–301. [CrossRef]
51. Hillert, M.; Jarl, M. A model for alloying effects in ferromagnetic metals. *Calphad* **1978**, *2*, 227–238. [CrossRef]
52. Dinsdale, A.T. SGTE data for pure elements. *Calphad* **1991**, *15*, 317–425. [CrossRef]
53. Lee, B.-J. Thermodynamic assessment of the Fe–Nb–Ti–C–N system. *Metall. Mater. Trans. A* **2001**, *32*, 2423–2439. [CrossRef]
54. Kolbasnikov, N.G.; Matveev, M.A.; Zotov, O.G.; Mishin, V.V.; Mishnev, P.A.; Nikonov, S.V. Physicochemical simulation of hot plasticity of microalloyed pipe steel in continuous casting and hot rolling. *Steel Transl.* **2014**, *2*, 59–64.
55. Suzuki, H.G.; Nishimura, S.; Yamaguchi, S. Characteristics of hot ductility in steels subjected to the melting and solidification. *Trans. ISIJ* **1982**, *22*, 48–56. [CrossRef]
56. Crowther, D.N. The effects of microalloying elements on cracking during continuous casting. In Proceedings of the Vanitec Symposium—The Use of Vanadium in Steel, Beijing, China, 12–14 October 2001; pp. 99–131. Available online: https://vanitec.org/images/papers/2001-The-Effects-of-Microalloying-Elements-on-Cracking-During-Continuous-Casting.pdf (accessed on 1 February 2023).
57. Lanjewar, H.A.; Tripathi, P.; Singhai, M.; Patra, P.K. Hot ductility and deformation behavior of C-Mn/Nb-microalloyed steel related to cracking during continuous casting. *J. Mater. Eng. Perform.* **2014**, *23*, 3600–3609. [CrossRef]
58. Yasumoto, K.; Maehara, Y.; Ura, S.; Ura, S.; Ohmori, Y. Effects of sulphur on hot ductility of low-carbon steel austenite. *Mater. Sci. Technol.* **1985**, *1*, 111–116. [CrossRef]
59. Kobayashi, H. Hot-ductility recovery by manganese sulphide precipitation in low manganese mild steel. *ISIJ Int.* **1991**, *31*, 268–277. [CrossRef]
60. Suzuki, H.G.; Nishimura, S.; Imamura, J.; Nakamura, Y. Embrittlement of steels occurring in the temperature range from 1000 to 600 °C. *Trans ISIJ* **1984**, *24*, 169–177. [CrossRef]
61. Hutchinson, C.R.; Zurob, H.; Sinclair, C.; Brechet, Y. The comparative effectiveness of Nb solute and NbC precipitates at impeding grain-boundary motion in Nb steels. *Scr. Mater.* **2008**, *59*, 635–637. [CrossRef]
62. Crowther, D.N.; Mintz, B. Influence of carbon on hot ductility of steels. *Mater. Sci. Technol.* **1986**, *2*, 671–676. [CrossRef]
63. Osinkolu, G.A.; Tacikowski, M.; Kobylanski, A. Combined effect of AIN and sulphur on hot ductility of high purity iron-base alloys. *Mater. Sci. Technol.* **1985**, *1*, 520–525. [CrossRef]
64. Harada, S.; Tanaka, S.; Misumi, H.; Mizoguchi, S.; Horiguchi, H. A Formation mechanism of transverse cracks on CC slab surface. *ISIJ Int.* **1990**, *30*, 310–316. [CrossRef]
65. Brune, T.; Senk, D.; Walpot, R.; Steenken, B. Hot ductility behavior of boron containing microalloyed steels with varying manganese contents. *Metall. Mater. Trans. B* **2015**, *46*, 1400–1408. [CrossRef]

66. Lankford, W.T. Some considerations of strength and ductility in the continuous-casting process. *Metall. Trans.* **1972**, *3*, 1331–1357. [CrossRef]
67. Carpenter, K.R.; Killmore, C.R.; Dippenaar, R. Influence of isothermal treatment on MnS and hot ductility in low carbon, low Mn steels. *Metall. Mater. Trans. B* **2014**, *45*, 372–380. [CrossRef]
68. Mintz, B.; Wilcox, R.; Crowther, D.N. Hot ductility of directly cast C–Mn–Nb–Al steel. *Mater. Sci. Technol.* **1986**, *2*, 589–594. [CrossRef]
69. Coleman, T.H.; Wilcox, J.R. Transverse cracking in continuously cast HSLA slabs—Influence of composition. *Mater. Sci. Technol.* **1985**, *1*, 80–83. [CrossRef]
70. Weinberg, F. The strength and ductility of continuously cast steels above 800 °C. *Metall. Trans. B* **1979**, *10*, 513–522. [CrossRef]
71. Crowther, D.N.; Green, M.J.W.; Mitchell, P.S. The influence of composition on the hot cracking susceptibility during casting of microalloyed steels processed to simulate thin slab casting conditions. *Mater. Sci. Forum* **1998**, *284–286*, 469–476. [CrossRef]
72. Ouchi, C.; Matsumoto, K. Hot ductility in Nb-bearing high strength low-alloy steels. *Trans. ISIJ* **1982**, *22*, 181–189. [CrossRef]
73. Mintz, B.; Arrowsmith, J.M. Hot-ductility behavior of C-Mn-Nb-Al steels and its relationship to crack propagation during the straightening of continuously cast strand. *Met. Technol.* **1979**, *6*, 24–32. [CrossRef]
74. Liu, Y.; Sun, Y.-h.; Wu, H.-t. Effects of chromium on the microstructure and hot ductility of Nb-microalloyed steel. *Int. J. Miner. Metall. Mater.* **2021**, *28*, 1011–1021. [CrossRef]
75. Abushosa, R.; Vipond, R.; Mintz, B. Influence of titanium on the hot ductility of as-cast steels. *Mater. Sci. Technol.* **1991**, *7*, 613–621. [CrossRef]
76. Chervonnyj, A.V.; Ringinen, D.A.; Astafev, D.S.; Efron, L.I. Investigation of hot ductility of microalloyed pipe steels produced at foundry-rolling complex. *Probl. Chern. Met. Materioloved.* **2015**, *2*, 49–56. Available online: https://www.elibrary.ru/item.asp?id=23592748 (accessed on 1 February 2023).
77. Koldaev, A.V.; D'yakonov, D.L.; Zaitsev, A.I.; Arutyunyan, N.A. Kinetics of the formation of nanosize niobium carbonitride precipitates in low-alloy structural steels. *Metallurgist* **2017**, *60*, 1032–1037. [CrossRef]
78. Rybkin, N.A.; Rodionova, I.G.; Shaposhnikov, N.G.; Kuznetsov, V.V.; Mishnev, P.A. Development of approaches for selecting the optimum alloying system and production parameters for manufacturing hot-rolled high-strength low-alloy steels for automobile building. *Metallurgist* **2009**, *53*, 486–494. [CrossRef]
79. Carpenter, K.R.; Dippenaar, R.; Killmore, C.R. Hot ductility of Nb- and Ti-bearing microalloyed steels and the Influence of thermal history. *Metall. Mater. Trans. A* **2009**, *40*, 573–580. [CrossRef]
80. Li, G.Y.; Li, X.F.; Ao, L.G. Investigation on hot ductility and strength of continuous casting slab for AH32 steel. *Acta Metall. Sin. Engl. Lett.* **2006**, *19*, 75–78. [CrossRef]
81. Zaitsev, A.I.; Koldaev, A.V.; Gladchenkova, Y.S.; Shaposhnikov, N.G.; Dunaev, S.F. Study and modeling of annealing regimes in bell furnaces for cold-rolled high-strength microalloyed steels. *Metallurgist* **2016**, *60*, 602–611. [CrossRef]
82. Lückl, M.; Wojcik, T.; Povoden-Karadeniz, E.; Zamberger, S.; Kozeschnik, E. Co-precipitation behavior of MnS and AlN in a low-carbon steel. *Steel Res. Int.* **2018**, *89*, 1700342. [CrossRef]
83. Mintz, B.; Abushosha, R. The influence of vanadium on hot ductility of steel. *Ironmak. Steelmak.* **1993**, *20*, 445–452. Available online: http://pascal-francis.inist.fr/vibad/index.php?action=getRecordDetail&idt=3908493 (accessed on 1 February 2023).
84. Banks, K.M.; Tuling, A.; Mintz, B. Influence of V and Ti on hot ductility of Nb containing steels of peritectic C contents. *Mater. Sci. Technol.* **2011**, *27*, 1309–1314. [CrossRef]
85. Chen, B.; Yu, H. Hot ductility behavior of V-N and V-Nb microalloyed steels. *Int. J. Miner. Metall. Mater.* **2012**, *19*, 525–529. [CrossRef]
86. Kim, S.K.; Kim, N.J.; Kim, J.S. Effect of boron on the hot ductility of Nb-containing steel. *Metall. Mater. Trans. A* **2002**, *33*, 701–704. [CrossRef]
87. Zarandi, F.; Yue, S. Effect of boron on the hot ductility of the Nb-microalloyed steel in austenite region. *Metall. Mater. Trans. A* **2006**, *37*, 2316–2320. [CrossRef]
88. Zarandi, F.; Yue, S. The effect of boron on hot ductility of Nb-microalloyed steels. *ISIJ Int.* **2006**, *46*, 591–598. [CrossRef]
89. Cho, K.C.; Mun, D.J.; Kim, J.Y.; Park, J.K.; Lee, J.S.; Koo, Y.M. Effect of boron precipitation behavior on the hot ductility of boron containing steel. *Metall. Mater. Trans. A* **2010**, *41*, 1421–1428. [CrossRef]
90. Cho, K.C.; Mun, D.J.; Kang, M.H.; Lee, J.S.; Kil Park, J.; Koo, Y.M. Effect of thermal cycle and nitrogen content on the hot ductility of boron-bearing steel. *ISIJ Int.* **2010**, *50*, 839–846. [CrossRef]
91. Shi, C.; Liu, W.; Li, J.; Yu, L. Effect of boron on the hot ductility of low-carbon Nb-Ti-microalloyed steel. *Mater. Trans.* **2016**, *57*, 647–653. [CrossRef]
92. Li, Q.; Liu, W. Effect of boron on hot ductility and room-temperature tensile properties of microalloyed steels with titanium and niobium. *Materials* **2019**, *12*, 2290. [CrossRef]
93. Komenda, J.; Luo, C.; Lönnqvist, J. Interaction of carbon, titanium, and boron in micro-alloy steels and its effect on hot ductility. *Alloys* **2022**, *1*, 133–148. [CrossRef]
94. Kolbasnikov, N.G.; Matveev, M. Research the influence of boron on hot ductility of microalloyed steels. *Glob. Energy* **2016**, *238*, 129–135. [CrossRef]
95. Liu, W.J.; Li, J.; Shi, C.B.; Huo, X.D. Effect of boron and titanium addition on the hot ductility of low-carbon Nb-containing steel. *HTMP* **2015**, *34*, 813–820. [CrossRef]

96. Gontijo, M.; Chakraborty, A.; Webster, R.F.; Ilie, S.; Six, J.; Primig, S.; Sommitsch, C. Thermomechanical and microstructural analysis of the influence of B- and Ti-content on the hot ductility behavior of microalloyed steels. *Metals* **2022**, *12*, 1808. [CrossRef]
97. Pereda, B.; Uranga, P.; López, B.; Rodriguez-Ibabe, J.M.; Stalheim, D.; Barbosa, R.; Rebellato, M.A. Through-thickness homogenization in thin slab direct rolling of Nb microalloyed steels. In Proceedings of the HSLA Steels 2015, Microalloying 2015 & Offshore Engineering Steels, Hangzhou, China, 11–13 November 2015; Springer: Cham, Switzerland, 2015. [CrossRef]
98. Li, X.; Li, Q.; Li, H.; Gao, X.; Deng, X.; Wang, Z. The Effect of cooling rate on the microstructure evolution and mechanical properties of Ti-microalloyed steel plates. *Materials* **2022**, *15*, 1385. [CrossRef]
99. Nie, Y.; Shang, C.J.; Song, X.; You, Y.; Li, C.; He, X.L. Properties and homogeneity of 550-MPa grade TMCP steel for ship hull. *Int. J. Miner. Metall. Mater.* **2010**, *17*, 179–184. [CrossRef]
100. Aichbhaumik, D. Steel variability effects on low cycle fatigue behaviour of high strength low alloy steel. *Metall. Trans. A—Phys. Metal. Mater. Sci.* **1979**, *3*, 269–278. [CrossRef]
101. Zaitsev, A.I.; Rodionova, I.G.; Arutyunyan, N.A.; Dunaev, S.F. Study of effect of non-metallic inclusions on structural state and properties of low-carbon microalloyed structural steels. *Metallurgist* **2021**, *64*, 885–893. [CrossRef]
102. Zaitsev, A.I. Prospective directions for development of metallurgy and materials science of steel. *Pure Appl. Chem.* **2017**, *89*, 1553–1565. [CrossRef]
103. Zaitsev, A.I.; Rodionova, I.G.; Baklanova, O.N.; Kryukova, A.I.; Udod, K.A.; Mishnev, P.A.; Mitrofanov, A.V. Nonmetallic inclusions and promising principles for Improving the set of properties and quality characteristics of steel. *Metallurgist* **2015**, *58*, 983–991. [CrossRef]
104. Lee, W.B.; Hong, S.G.; Park, C.G.; Kim, K.H.; Park, S.H. Influence of Mo on precipitation hardening in hot rolled HSLA steels containing Nb. *Scr. Mater.* **2000**, *43*, 319–324. [CrossRef]
105. Koldaev, A.V.; Arifulov, F.V.; Zaitsev, A.I.; Arutyunyan, N.A.; Alexandrova, N.M. Effect of excess phase precipitation on strengthening of structural steels prepared by hot stamping. *Metallurgist* **2020**, *64*, 438–445. [CrossRef]